Approaches to estimate global safety factors for reliability assessment of RC structures using non-linear numerical analyses

Engineering Structures 311 (2024) 118193

Contents lists available at ScienceDirect

Engineering Structures

journal homepage: www.elsevier.com/locate/engstruct

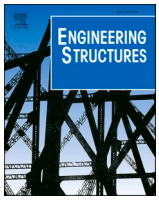

Approaches to estimate global safety factors for reliability assessment of RC structures using non-linear numerical analyses

Elena Miceli, Diego Gino *, Paolo Castaldo

Department of Structural, Geotechnical and Building Engineering (DISEG), Politecnico di Torino, Turin, Italy

ARTICLE INFO

Keywords:
Non-linear numerical analysis
Safety assessment
Global safety factors
Reinforced concrete
Dominant and non-dominant variables

ABSTRACT

The study is focused on the comparison and discussion of different approaches within the use of the global resistance method (GRM) for safety assessment of reinforced concrete (RC) systems using non-linear numerical analyses (NLNAs). With this purpose, a benchmark dataset, comprising 56 experimental results obtained from tests on 40 RC columns with variable slenderness and 16 non-slender RC elements including walls, deep beams and shear walls, is considered. The NLN models for all the 56 members adopt solution strategies able to optimize the agreement between numerical predictions and experimental outcomes. Then, probabilistic hypotheses have been defined regarding both aleatory (i.e., materials and geometry) and epistemic uncertainties (i.e., model) associated with all the 56 RC members. These assumptions form the basis for developing a comprehensive set of probabilistic analyses of the global structural resistance for each RC member. The results of these probabilistic analyses offer valuable insights into the impact of the different sources of uncertainties on the global structural response. In detail, three distinct approaches for estimating the global safety factors within the GRM are outlined and compared. The purpose is to address the effectiveness of the different approaches for the reliability evaluation of RC members within the GRM together with the relevance of both aleatory and epistemic uncertainties. Ultimately, recommendations are provided regarding the adoption of the GRM in the upcoming generation of design codes.

1. Introduction

Non-linear numerical analyses (NLNAs) have revolutionized structural engineering, particularly, in the design and assessment of new and existing reinforced concrete (RC) structures [1–3]. With the evolution of computer-assisted design tools, NLNAs are increasingly used for complex and detailed structural evaluations [4–8], gradually supplementing traditional and analytical methods for safety assessment [9,10]. This progress is backed by various guidelines and methodologies [11,12], and the next generation of design codes [13] is expected to incorporate these advanced methods, highlighting the need for comprehensive research with respect to both limits of applicability and uncertainties [14–16]. NLNAs excel in analysing RC structures with variable geometries, such as buildings with irregular floor configurations, and can address challenges like mechanical and geometrical non-linearities, detailing deficiencies and localized damages [17–22]. These analyses are also crucial in evaluating the impact of interventions on existing bridges or buildings, particularly, on elements like piers or columns that experience geometrical non-linearity [23].

The reliability analysis of RC structures can be conducted using various formats capable of incorporating both aleatory (i.e., materials, geometrical properties and actions) and epistemic (i.e., modelling) uncertainties, as outlined in [9,10], primarily including the *probabilistic format* (PF), *partial safety factors format* (PSFF) and *global resistance format* (GRF). The PF aims to directly estimate the probability of failure [24,25], assuming specific probabilistic distributions for both aleatory and epistemic uncertainties. In contrast, the PSFF assigns design values to variables associated with material properties, geometry, actions, and related effects, thereby allowing for local safety verifications [14] of members resistance (i.e., semi-probabilistic method) [26,27]. The GRF treats uncertainties related to actions similarly to the PSFF, while addressing uncertainties related to structural response at a global level [14] conducting global safety verification. Specifically, the GRF approach [10] facilitates direct comparison between the design actions [28] and global design resistance of a structure, incorporating both aleatory (i.e., related to materials and geometrical properties) and epistemic uncertainties (i.e., related to assumptions for numerical model definition) [14,29]. Within the philosophy of the global resistance format, the global resistance method (GRM) [10–14,29] is one of the

* Corresponding author.
E-mail address: diego.gino@polito.it (D. Gino).

https://doi.org/10.1016/j.engstruct.2024.118193
Received 14 February 2024; Received in revised form 19 April 2024; Accepted 12 May 2024

Nomenclature

R_{Gl}	global structural resistance random variable inclusive of both aleatory and epistemic uncertainties
R	global structural resistance random variable inclusive of aleatory uncertainties only
R_d	design value of global structural resistance
R_{NLNA}	value of global structural resistance achieved using non-linear numerical analyses
f	material property random variable
f_{rep}	representative value of material property (i.e., experimental, f_{Exp}; mean, f_m)
a	geometric property random variable (i.e., experimental, a_{Exp}; nominal, a_n)
ϑ	model uncertainty random variable ("pure" or "actual" value - deprived of the experimental uncertainty)
μ_ϑ	mean value of model uncertainty random variable ("pure" or "actual" value - deprived of the experimental uncertainty)
V_ϑ	coefficient of variation of model uncertainty random variable ("pure" or "actual" value - deprived of the experimental uncertainty)
ϑ_{obs}	model uncertainty random variable ("observed" value)
$\mu_{\vartheta,obs}$	mean value of model uncertainty random variable ("observed" value)
$V_{\vartheta,obs}$	coefficient of variation of model uncertainty random variable ("observed" value)
F_d	design value of an action or set of actions under the relevant combination
γ_{Gl}	global safety factor
γ_{Gl}^{I}	estimation of global safety factor using *Approach I*
$\gamma_{Gl}^{I/b}$	estimation of global safety factor using *Approach I/b*
γ_R	global resistance safety factor
γ_{Rd}	model uncertainty safety factor
γ_{Gl}^{II}	estimation of global safety factor using *Approach II*
β_t	target value of the reliability index
α_R	first-order reliability method (FORM) factor assuming dominant variable
α'_R	first-order reliability method (FORM) factor assuming non-dominant variable
δ_{Gl}	bias factor associated with global structural resistance
δ_{Gl}^{II}	estimation of bias factor associated with global structural resistance using *Approach II*
δ_R	*mean-to-mean* deviation ratio
δ_ϑ	model uncertainty bias factor
V_{Gl}	coefficient of variation of global structural resistance
V_{Gl}^{II}	estimation of coefficient of variation of global structural resistance using *Approach II* (a and b)
V_R	coefficient of variation of global structural resistance considering only aleatory uncertainties
λ	slenderness of the RC column
$\varepsilon_{s,max}$	maximum strain in "primary reinforcement" estimated through NLNAs
ε_y	yielding strain of "primary reinforcement"

preferred safety formats used for practical purposes. As described in next section, the GRM allows to estimate the design value of the global resistance of a structure (i.e., global structural resistance), by means of a limited number of numerical simulations, and accounts for both aleatory and epistemic uncertainties through the definition of "global safety factors" [10]. In this way, the global safety factors are applied at a global level in terms of structural response to ensure that structural systems meet safety requirements. Specifically, the global safety factors are used to reduce the global structural resistance estimated by NLNAs to account for uncertainties [14,30] in accordance with specific reliability levels [10,31,32]. The global safety factors can be estimated through the assessment of statistical parameters related to the probabilistic distribution of global structural resistance including the influence of both the aleatory and epistemic uncertainties [10–14,33]. In this framework, two main philosophies can be recognized [10,14,30] to compute the global safety factors:

i) the adoption of separate global safety factors for aleatory and epistemic uncertainties denoted, respectively, as *global resistance safety factor* and *model uncertainty safety factor;*
ii) the adoption of a single *global safety factor* able to include both aleatory and epistemic uncertainties.

Referring to the first philosophy (i.e., case i)), it is based on the assumptions provided in [34,35], which establish a set of fixed values for the first order reliability method (FORM) factors related to resistances (i.e., α_R) and action variables (i.e., α_E). These predefined values are intended to be applicable to a significant portion of situations related to structural applications. The aim is to facilitate the practical use of the semi-probabilistic method in engineering practice, as discussed in [10] and [28]. According to [10,34,35], the primary focus is to assume aleatory uncertainties as the dominant ones, while epistemic uncertainties as non-dominant resistance variables. Although it should be theoretically examined case-by-case, this approach typically ensures a safe evaluation of structural resistance in practical applications [10].

On the contrary, the use of a single global safety factor (i.e., case ii)) offers some advantages. In fact, it ensures a more consistent incorporation of both aleatory and epistemic uncertainties when evaluating the design value of global structural resistance. Moreover, this approach eliminates the need to make assumptions about the dominance or non-dominance of either type of uncertainty, as discussed in [36].

The present study involves a comprehensive analysis of the approaches related to the application of the GRM and associated global safety factors for the safety assessment of RC systems through NLNAs. Specifically, it proposes novel insights into the integration of both aleatory and epistemic uncertainties in structural reliability evaluation. To accomplish this objective, a substantial dataset comprising 56 experimental results from tests conducted on different RC members is considered. This dataset encompasses 40 RC columns [37–45] with varying slenderness ratios and 16 non-slender RC elements, including deep beams and walls [46–49]. NLN models are defined for all the 56 RC elements, with a strong focus on formulating effective solution strategies to enhance the alignment between numerical predictions and actual experimental results also grounding on the experience from previous researches [14,29,50,51]. Additionally, probabilistic hypotheses [52] are established to account for both aleatory (i.e., random variables related to materials and geometry) and epistemic (i.e., modelling assumptions in defining the numerical models) uncertainties. These assumptions serve as the basis for extensive probabilistic analyses aimed at assessing the global structural resistance of each RC element. The results of these probabilistic analyses offer valuable insights into the influence of both the uncertainty sources on the structural response. In detail, three distinct approaches for estimating the global safety factors within the framework of the GRM are delineated and compared. The primary objective is to determine the effectiveness of the approaches for the reliability evaluation of RC members within the GRM together with the relevance of both aleatory and epistemic uncertainties.

Ultimately, drawing inspiration from the ongoing process of updating the current design codes, e.g. [13] and [53], this study offers recommendations regarding the integration of the GRM into next

generations of design codes. Specifically, it provides contributions to the advancements in both the safety assessment and design practices of RC structures.

2. Global resistance method for safety evaluation of RC structures by means of NLNAs

This section deals with the fundamental concept of the GRM [10] for safety verification of RC members using NLNAs. Subsequently, it outlines potential approaches to implement the GRM, along with the corresponding estimation of the global safety factors.

2.1. Basic principles

The GRM is a safety format based on the principles of the global resistance format, initially introduced by [10] and further investigated by [14,15,29,30,33]. Essentially, it enables safety verifications by estimating the global structural resistance that the system provides against a set of concurrent external actions [14]. The advantage of using a global approach, as opposed to a local one [14], is the ability to comprehensively address behavior of structural systems by exploiting the capabilities of non-linear numerical tools. This includes ultimate capacity, progressive damage, ductility and redistribution of internal stresses in non-linear field, encompassing both geometrical and mechanical non-linearities [17,18]. Generally, the global structural resistance (R_{Gl}) is described as a random variable dependent on both aleatory (i.e., materials (f) and geometrical (a)) and epistemic (i.e., model (ϑ)) uncertainties and can be represented [54] as follows:

$$R_{Gl} = R_{Gl}(f, a;\ \vartheta) \tag{1}$$

The characterization of the random variable representing the global structural resistance (R_{Gl}) can be achieved through NLNAs, considering the different uncertainties through probabilistic analyses [29,30]. However, for practical purposes, methods capable of conducting reliability assessments without running full probabilistic simulations are needed. Essentially, the GRM [10,29] is conceived for practical applications of NLN methods and enables global structural verification, estimating the design value (R_d) of the global structural resistance, using Eq.(2):

$$R_d = \frac{R_{NLNA}\left(f_{rep}, a_{rep}\right)}{\gamma_{Gl}} \geq F_d \tag{2}$$

In Eq.(2), R_{NLNA} represents the global structural resistance estimated by NLNAs using representative values of materials (f_{rep}) and geometrical properties (a_{rep}). Meanwhile, γ_{Gl} represents the global safety factor capable of accounting for the influence of aleatory (i.e., materials and geometrical properties) and epistemic (i.e., model) uncertainty [55,56] with respect to desired target reliability [10,31,32]. The term F_d represents the design value of the actions, assessed in accordance with the specified combination as outlined in [28].

With reference to the aleatory uncertainties, these are represented by the inherent randomness of the materials and geometrical properties [14,29] that can be characterized by appropriate probabilistic distributions (e.g., normal or lognormal).

Regarding the epistemic uncertainties, these arise from model uncertainty associated with the choices made by the analyst in defining the numerical model for NLNAs [50,55,57,58,56]. These choices encompass all the modeling assumptions related to equilibrium evaluation, kinematic compatibility of displacements and constitutive laws for materials [50,55,57,58,56]. In fact, different assumptions related to the mentioned above aspects would lead to different results in terms of R_{NLNA}. For instance, the model uncertainty should account for the uncertainty linked to various sets of modeling assumptions potentially used by different analysts to investigate the behavior of a specific RC member (i.e., "between" model uncertainty) and the use of a single set of modeling assumptions employed by the same analyst to study different structural members (i.e., "within" model uncertainty) [56]. The epistemic uncertainty is typically represented by lognormal probabilistic distribution [55,57,58,56] and, for practical purposes, it should be deprived of the experimental uncertainties [50,56].

The estimation of R_{NLNA} in Eq.(2) should be carried out through NLNAs, adopting the appropriate loading arrangement consistent with the set of actions simultaneously affecting the structure in the specific design combination F_d [28]. Regarding the values of f_{rep} and a_{rep}, the GRM adopts these values as equal to the corresponding mean (f_m) and nominal (a_n) ones [14–16,24,25–27,59,17–23,28,29,30]. This choice is supported by various investigations [14,15,29,30], demonstrating that the value of $R_{NLNA}(f_m,a_n)$ can effectively approximate the mean value of the global structural resistance derived from a probabilistic evaluation with a high degree of accuracy. Additionally, it is capable to account for the structural response through the most likely failure mode [14,51] within the safety evaluation. The uncertainty associated with further potential failure modes due to different combinations of the representative values f_{rep} and a_{rep} [14], especially for RC systems [27], can be addressed by conducting a probabilistic analysis to assess γ_{Gl}. Otherwise, in the case of simplified safety formats suitable for practical purposes [10–15] (e.g., partial factor method – PFM [10], estimation of coefficient of variation method – EcoV [10]), the value of γ_{Gl} should be increased by 1.15 when the "non-decreasing assumption" [27] for the response surface of structural resistance with respect to basic variables is not satisfied, as outlined in [13,14] and [27].

It is worth noting that in the circumstance of reproducing experimental tests through NLNAs, if data are available from original reports, the values of f_m and a_n can be assimilated to the corresponding experimental observations f_{Exp} and a_{Exp} [14,29]. This assumption is accepted throughout the present investigation. The safety verification described in Eq.(2) can be aligned with pre-determined target reliability levels, making a distinction between new and existing structures [10,28,31,32] by calculating the related value of the global safety factor (γ_{Gl}). The following subsection describes the three approaches to assess the global safety factor.

2.2. Approaches to determine the global safety factor

The estimation of the global safety factor (γ_{Gl}) should be carried out including the contribution of both aleatory (i.e., materials and geometry) and epistemic (i.e., model) uncertainties [10,14,15,53,60,61]. In line with [10,29,30,33,53,58,62], the available approaches to calculate γ_{Gl} can be summarized within the following three methodologies denoted as *Approach I*, *II* and *III*.

Approach I aligns with *fib* Model Code 2010 [10], which distinguishes between partial safety factors for aleatory uncertainties (γ_R) (i.e, *global resistance safety factor*) and epistemic uncertainties related to the definition of the numerical model (γ_{Rd}) (i.e., *model uncertainty safety factor*). Based on these considerations of *Approach I*, the value of γ^{I}_{Gl} can be estimated as:

$$\gamma^{I}_{Gl} = \gamma_R \cdot \gamma_{Rd} \geq 1.00 \tag{3}$$

In Eq.(3), the values of γ_R and γ_{Rd} can be determined assuming a lognormal probabilistic distribution for both sources of uncertainty [10,29,30,56]. Moreover, the assumption that the aleatory uncertainties are dominant resistance variables within the reliability evaluation of the system is generally accepted in the evaluation of γ_R and γ_{Rd} according to [10,14,29,53,55,57,58,56]. It means that epistemic uncertainties, in this case, are assumed as non-dominant resistance variables in their contribution to overall reliability of the system.

The value of γ_R applies:

$$\gamma_R = \frac{\exp(\alpha_R \cdot \beta_t \cdot V_R)}{\delta_R} \geq 1.00 \tag{4}$$

where β_t is the target value of the reliability index [10,31,32]; α_R denotes the FORM sensitivity factor assumed equal to 0.80 in the hypothesis of dominating aleatory uncertainties [10,34] with respect to the epistemic ones. The term V_R denotes the coefficient of variation (CoV) of the global structural resistance, assumed to follow a lognormal distribution and related to the aleatory uncertainties (i.e., materials and geometrical properties) [10–14,53,56]. The term δ_R is the ratio between the mean value of structural resistance, estimated by means of probabilistic analysis including aleatory uncertainties only (μ_R), and $R_{NLNA}(f_m,a_n)$. δ_R is associated with both material and geometrical properties and represents the bias factor between the result from one NLNA represented by $R_{NLNA}(f_m,a_n)$ in comparison to the mean value of the global structural resistance obtained through a probabilistic analysis (i.e., *mean-to-mean* deviation) [29]. The values of both V_R and δ_R can be assessed by means of probabilistic analysis of the global structural resistance including aleatory uncertainties only (i.e., materials and geometry) [29]. For practical application of the GRM, V_R and δ_R can be approximated according to simplified methods [29,51] within safety formats [10,14,15], without the need to carry out a complete probabilistic investigation.

Instead, the value of γ_{Rd} can be computed as follows:

$$\gamma_{Rd} = \frac{\exp(\alpha_R' \cdot \beta_t \cdot V_\vartheta)}{\delta_\vartheta} \geq 1.00 \tag{5}$$

In Eq.(5), β_t has the same meaning as in Eq.(4), α'_R represents the FORM factor, set equal to 0.32 in accordance with the assumption that aleatory uncertainties dominate over epistemic ones [10,34]. Following [53,50,57,58,56], the random variable ϑ, which represents the model uncertainty, can be characterized through statistical analysis of the ratio between the experimental global structural resistance and numerical one, considering both "between" and "within" model variabilities. As already introduced, such uncertainties should be deprived of the experimental uncertainties related to tests and measurement errors [29, 56,63]. In Eq.(5), V_ϑ represents the CoV of the model uncertainty random variable ϑ, while δ_ϑ corresponds to the associated bias factor [53,50,57,58,56]. The bias factor for model uncertainty, δ_ϑ, is typically equal to the mean value (μ_ϑ) of the probabilistic distribution associated with the model uncertainty (ϑ) [53,50,57,58,56]. Note that, for practical purposes and in cases in which the statistical characterization of the random variable ϑ is not possible, appropriate values of γ_{Rd} should be adopted, as discussed in [53,50,57,58,56].

This approach (*Approach I*), although widely adopted [10], requires the identification of the dominant source of uncertainty (i.e., aleatory or epistemic) influencing the random variability of the global structural resistance variable (R_{Gl}) for the reliability analysis. In general applications, the assumption of dominant aleatory uncertainties with respect to the epistemic ones leads to safe evaluations of R_d [10,15,56] even if it is recommended to check the truthfulness of this assumption [58,64].

Approach II allows for the direct estimation of the *global safety factor* γ^{II}_{Gl} by means of Eq.(6), always in agreement to the assumption of lognormal distribution for the global structural resistance [10,29,30,36, 53,56]:

$$\gamma^{II}_{Gl} = \frac{\exp\left(\alpha_R \cdot \beta_t \cdot V^{II}_{Gl}\right)}{\delta^{II}_{Gl}} \geq 1.00 \tag{6}$$

where α_R represents the FORM sensitivity factor, assumed to be 0.80 under the assumption of a dominant resistance variable that, in this case, refers to both aleatory and epistemic uncertainties. The values of V^{II}_{Gl} and δ^{II}_{Gl} denote, respectively, the CoV and bias factor related to the global structural resistance (R_{Gl}), considering the contribution of both aleatory and epistemic uncertainties. These values can be estimated using the following simplified expressions [36]:

$$V^{II}_{Gl} = \sqrt{V_R^2 + V_\vartheta^2} \tag{7}$$

$$\delta^{II}_{Gl} = \delta_R \cdot \delta_\vartheta = \delta_R \cdot \mu_\vartheta \tag{8}$$

In Eq.s (7)-(8), the values of V_R, V_ϑ, δ_R and δ_ϑ (as well as μ_ϑ) assume the same meaning as described in the previously outlined *Approach I*. Compared to *Approach I*, *Approach II* does not necessitate any assumptions regarding the dominant or non-dominant role of aleatory uncertainties over epistemic ones or vice versa. The contribution to overall reliability of the RC system from both the sources of uncertainty is considered through their statistical parameters in Eq.s (7)-(8).

Approach III is herein conceived to assess the effectiveness of both *Approach I* and *Approach II* in determining the actual safety level within global verifications. *Approach III* involves estimating the global safety factor γ_{Gl} according to Eq.(6), but with a more precise assessment of the CoV V_{Gl} and bias factor δ_{Gl} associated with the global structural resistance. Unlike the other approaches, these can be exclusively computed through a comprehensive probabilistic analysis of the global structural resistance (R_{Gl}). This analysis includes the sampling of both aleatory (i. e., material and geometric) and epistemic (i.e., model) uncertainties for the direct characterization of the global resistance random variable, as indicated in Eq.(1) [54,65]. *Approach III* represents the most accurate approach and is adopted as the reference one.

Finally, in the mentioned approaches, the use of Eq.s (4)-(8) can be considered valid as long as the CoV values of the main variables remain equal or lower than 0.3, with an error margin of around 5% [36]. If this is not the case, full expressions based on the assumption of lognormal distributed variables can be derived according to [65].

Next, a comparison of the three approaches is presented, employing NLN models calibrated on experimental results of RC members with different characteristics.

3. Benchmark experiments, non-linear numerial models and probabilistic analysis

This section reports a description of the benchmark set of experimental tests [37–49] considered in this study, accompanied by the modeling assumptions for NLNAs and probabilistic characterization of the relevant aleatory and epistemic uncertainties.

3.1. Set of benchmark experiments

This subsection provides a concise description of the experimental tests used to validate the numerical models with the aim to conduct a comprehensive probabilistic analysis of the global structural resistance [11,26] and compare the three approaches for deriving γ_{Gl}, as insights for the next generation of design codes. As highlighted in [50], the selection of the experimental tests should adhere to specific criteria, considering material properties (e.g., concrete cylinder compressive strength (f_c), steel reinforcement grade related to yielding strength in tension (f_y)) and geometrical properties (e.g., minimum size of the members, minimum and maximum reinforcement ratios) to respect the limits of applicability defined in the design codes. This investigation adopts the limits of applicability outlined in EN1992 [9] and *fib* Model Code 2010 [10], where the GRM has been implemented for safety verifications through NLN methods. Note that many of these limitations partially align also with the specifications of other worldwide recognized codes, such as ACI 318 [66]. More specifically, the main reinforcement has to respect a minimum diameter (Φ_l) of 8 mm, with the minimum reinforcement area set at 0.002 times the area of the cross-sections (A_c), and a maximum reinforcement area of 0.04 times A_c. Regarding transversal reinforcement, the minimum diameter is determined as the maximum value between 0.25 times the longitudinal reinforcement diameter (Φ_l) and 6 mm, while the maximum spacing is calculated as the minimum value between 20 times Φ_l, the member width (b), the height (h) and 400 mm. Moreover, specific provisions state that every longitudinal bar, located in a corner, must be supported

by transverse reinforcement, and no bar within a compression zone should be positioned more than 150 mm away from a restrained bar.

According to the previous considerations, the benchmark set of experimental results comprises two distinct families of tests:

- 40 RC columns with increasing slenderness, tested by [37–45] (i.e., *slender members*);
- 16 RC members, including deep beams and walls with various geometry and loading configurations, investigated by [46–49] (i.e., *non-slender members*).

The experimental results collected by [50] from [37–45] have been selected as *slender members* consisting of 40 RC columns. This selection has been based on their conformity to the limitations defined in [9,10], with the objective of achieving an homogeneous representation of both the geometrical and materials properties. In [50], experimental results from short-term compression tests have been exclusively considered, disregarding any long-term influence of creep. For the slenderness (λ), a broad range of values, from 15 (i.e., ordinary slender members) to approximately 280 (i.e., extremely slender members), has been considered. The experimental concrete compressive strength of the specimens has been obtained from [19] and varies between 15–60 MPa,

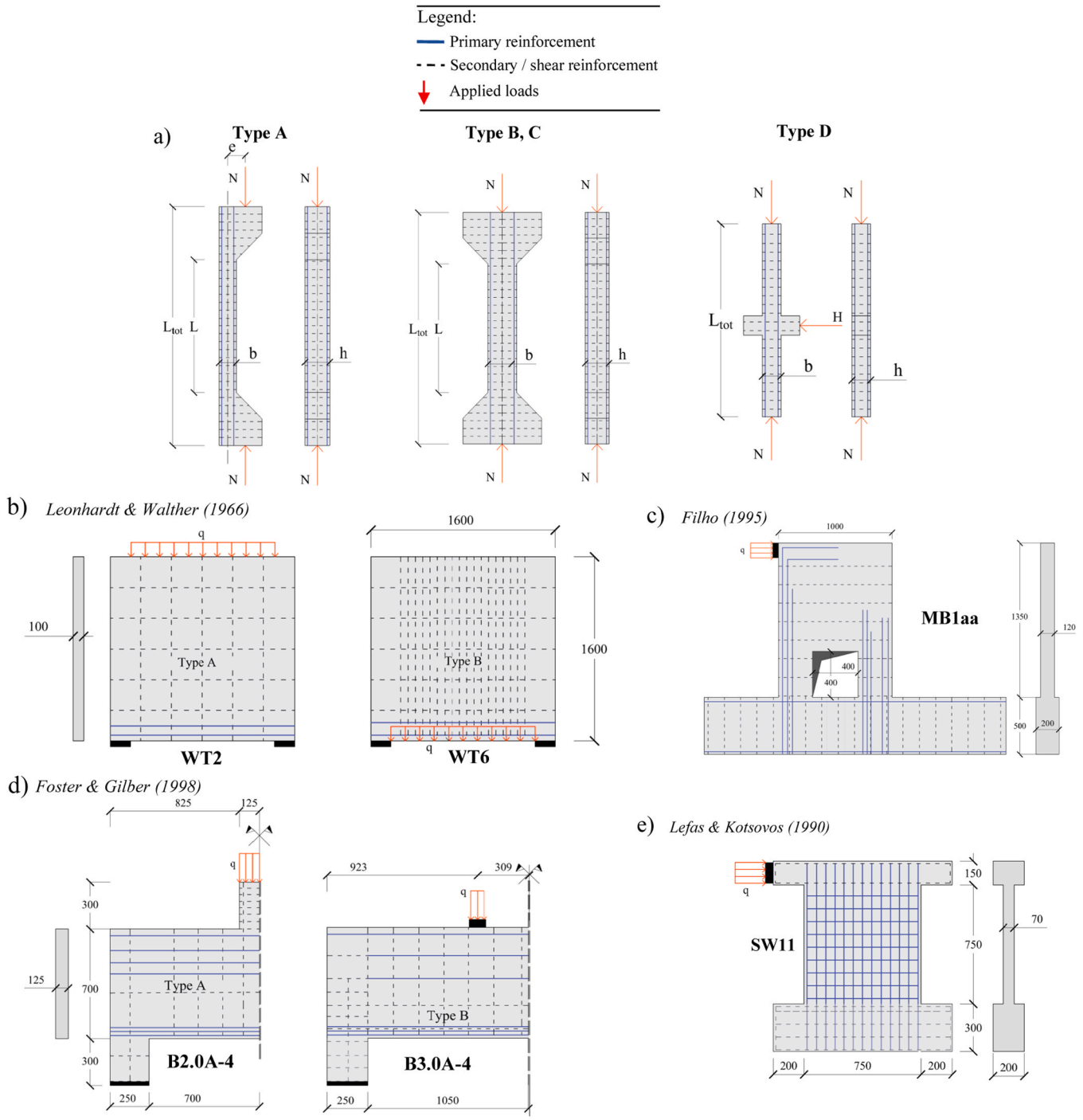

Fig. 1. Representation of the general features related to the *slender members* selected by [50] from [37–45] and of the *non-slender members* selected from [46–49]. Dimensions are in millimetres.

representative of normal strength classes for concrete (i.e., lower than C50/60 according to [9]). The experimental value of the yielding strength for reinforcement reflects properties of steel according to grades 300, 400 and 500 MPa. The longitudinal reinforcement ratio (i.e., total longitudinal reinforcement over concrete area) is within the range of 0.2–4%. The static schemes related to the experimental tests of [37–45] can be categorized into four different configurations denoted as *Type A*, *B*, *C* and *D* schemes [50], shown in Fig. 1(a). Detailed information about testing procedures, geometrical and material properties can be acknowledged in [50], as well as in [37–45]. The slenderness (λ) of the RC columns, with rectangular cross-section, is computed as $\sqrt{12}L/h$ [50].

Concerning the 16 experimental results of RC *non-slender members* [46–49], the selection aims for a balanced range of material properties within the limits specified in design codes [9,10] and covers the transition from brittle to ductile failure modes [51,55]. These members have been configured with an isostatic restraint scheme and loaded according to protocols detailed in [46–49].

From [46], experiments on five deep beams (WT2, WT3, WT4, WT6, WT7) have been considered. These beams, 1.6 m wide and 1.6 m high with a uniform thickness of 0.10 m, featured various reinforcement configurations. Two types of loading configurations are considered as showed in Fig. 1(b) (denoted as *Type A* – WT2, WT3, WT4 and *Type B* – WT6, WT7). The cylinder compressive strength of the concrete varies across different tests, ranging from 26.7 to 28.7 MPa. Meanwhile, the mechanical properties of the reinforcement depend on the diameter of the bars. The failure modes ranged from concrete crushing with longitudinal bar yielding to concrete crushing at the side of the cross-section without appreciable yielding.

In [47], experiments on several RC deep beams were conducted and five of them have been herein considered (B2.0–1, B2.0–3, B3.0–1, B2.0A-4, B3.0A-4). The RC deep beams measure 0.7 m in depth and 0.125 m in thickness. Different geometries characterize the five RC members, which can be grouped into *Type A* and *Type B*, as shown in Fig. 1(d). The concrete cylinder compressive strength varies between 78 and 88 MPa in the different tests. The beams differed in load arrangements, showing distinct failure modes, such as concrete crushing at the edge of the loading column or in the main body of the wall.

From the study of [48], five RC walls with openings (MB1aa, MB1ae, MB1ee, MB1ee1, MB4ee), having similar geometrical properties but different reinforcement layouts, have been considered (Fig. 1(c)). The concrete cylinder compressive strength varies from 39 to 42 MPa in the different tests. The walls exhibited brittle or nearly brittle responses, forming inclined compression struts and concrete crushing at the connection to the stiff foundation.

Finally, the RC wall SW1 of [49] has been considered with dimensions of 1.2 m in height, 0.75 m in width and 0.07 m in thickness (Fig. 1(e)). The concrete cylinder compressive strength is equal to 43 MPa. The observed failure mode involved inclined cracks within the wall, accompanied by concrete crushing at the compressed edge and reinforcement yielding on the opposite tensile side. Fig. 1(b)-(c) shows the main features of the selected members [46–49]. Details regarding the testing procedures, geometrical configurations and materials properties may be found in [46–49].

In the next, the basic hypotheses related to the NLN modeling of both the *slender* and *non-slender members* are presented.

3.2. Assumptions for NLN modelling and suitability for probabilistic analysis

In this subsection, the main assumptions related to the definition of the NLN models representing the 40 RC *slender members* [37–45] and 16 RC *non-slender members* [46–49] are outlined. In line with [10,12,50,55,57,58,56,67,68], the assumptions have been developed to encompass considerations for material constitutive laws, kinematic compatibility and assessment of equilibrium between internal and external forces. The NLN models have been developed in such a way as to closely match the experimental outcomes with the numerical results, using experimental values (herein assumed as mean values) for geometrical (a_{Exp}) and material (f_{Exp}) properties [14,24]. In agreement with [14,24], this investigation adopts modelling assumptions aimed to minimize the discrepancy between experimental and numerical results [50,55,57,58,56]. According to [14,29,51], this is crucial to make the NLN model suitable for conducting accurate and reliable probabilistic analyses, as discussed in next sections.

With reference to the 40 RC *slender members* [37–45], the assumptions for defining the NLN models have been summarized in Table 1, as referenced by [50] and [29]. The Opensees [69] software platform has been employed for this purpose, adopting a fiber-modelling approach. This approach notably features distributed plasticity and addresses both mechanical and geometrical non-linearities and well fits the need to model RC columns with relevant slenderness [50]. According to [50], the RC columns have been modelled with the main body exhibiting non-linear behaviour, while larger regions placed close to loading devices have been represented with an elastic behaviour, as also detailed in Table 1. Non-linear regions have been modelled using force-based fiber beam-columns elements according to [69]. The non-linear cross-sections have been defined with optimum fiber-mesh subdivision equal to 40×40 distinguishing between fibers pertaining to concrete cover (un-confined), concrete core (confined) and reinforcement [50]. Elastic beam-column elements [69] have been used for regions of the columns not affected by non-linear behaviour. Details about the adopted constitutive laws for concrete, confined concrete and reinforcements are reported in Table 1. Specifically, Table 1 reports the optimum set of modelling assumptions in line with [50].

The NLN models for 16 RC *non-slender members* [46–49] have been developed using specific assumptions within ATENA 2D [73] software platform. In line with Table 2, these members have been represented by quadrilateral plane stress finite elements (CCQ10SBeta [73]) with

Table 1
Assumptions for NLN modelling of the 40 RC *slender members* of [37–45] in line with [50].

***Slender members*: Opensees** [64]	
Equilibrium of forces	• The full Newton-Raphson has been used as iterative method [11] to solve the non-linear system of equations; • Each iteration considered the deformed configuration, accounting for the second-order effects through the *P-delta geometric transformation* [69], with a maximum of 200 iterations per load step; • Displacements based convergence criteria, with a tolerance of 1%; • Incremental Load Steps: determined with respect to both experimental execution and numerical calibration for an optimal numerical accuracy.
Kinematic compatibility	• *Fiber Beam-Column Elements*: a force-based approach [69] is used for cross-sections exhibiting non-linear responses [50], employing a 40×40 fiber-grid subdivision; • *Elastic Beam-Column Elements:* applied for cross-sections demonstrating elastic responses [50,69].
Constitutive relationships	• *Concrete (non-linear cross-sections)*: implemented the *Concrete02* model [69]: *Compression behaviour*: mono-axial non-linear model has been used for both un-confined and confined concrete, following [70]; *Tension behaviour*: it has been modelled using elastic behavior with a post-peak Linear Tension Softening (LTS) law, which has been calibrated to match the experimental results; • *Reinforcements (non-linear cross-sections)*: it has been employed the ReinforcingSteel model [69] adopting elastic behaviour with curvilinear hardening in line with [71] incorporating a buckling model based on [72]. *Further observations about materials properties*: defined in accordance with data from the original research papers [37–45] and, if data are missing, compliant with the standards outlined in [9].

Table 2
Assumptions for NLN modelling of the 16 RC *non-slender members* of [46–49] in line with [51].

***Non-slender members*: ATENA 2D**[73]	
Equilibrium of forces	• Nonlinear system of equations solved using the standard Newton-Raphson iterative approach with "line search" [11]; • Max iteration limit: 200; • Convergence criteria: 1% (forces) and 0.01% (energy); • Loading procedure follows experimental one: initial dead load application, then incremental experimental actions until failure. Load steps sized for accuracy and computational effort.
Kinematic compatibility	• Body of the RC members represented by quadrilateral plane stress finite elements (CCQ10SBeta [73]) with quadratic displacement interpolation functions [73]; • Reinforcement representation by smeared approach for secondary, wall and shear reinforcement; discrete approach for primary reinforcement [11,73]; • Mesh size calibrated for each element, ranging between 5 and 10 cm. Aimed to balance accuracy and computational effort [12].
Constitutive relationships	• *Concrete*: SBeta material model [73] for non-linear behavior of concrete under compression and tension. *Compression behaviour*: curvilinear response with linear compression softening (LCS), calibrated for 50% reduction in strength post-peak load at reaching the ultimate strain; *Tension behaviour*: elastic until tensile strength is reached, with post peak linear tension softening (LTS), calibrated for ultimate strain at zero stress equal to 2-10 times the strain in concomitance of the peak tensile strength [58]; *Cracking*: smeared crack modelling with the rotated crack model [11,73]. • *Reinforcement*: bilinear constitutive model with hardening law for both compression and tension. Properties determined from experimental findings [46–49]. If data are not available, Young's modulus: 210000 MPa, ultimate strain ε_u: 9% [29]. *Further observations about materials properties*: based on the experimental data [46–49]. Missing parameters adopted according to [9].

quadratic displacement interpolation functions. The mesh size for each element has been calibrated between 5 and 10 cm, balancing accuracy and computational effort [12]. The non-linear equations have been solved using the standard Newton-Raphson method with the convergence criteria reported in Table 2. The constitutive models for concrete behaviour under compression and tension have been simulated using the SBeta material model [73]. This model accounts for both curvilinear compression response with linear compression softening (LCS) and elastic tensile behaviour with linear tension softening (LTS). The LCS law ensures a 50% reduction in compressive strength after peak load attaining the ultimate stain in compression, while the LTS law optimizes predictions compared to experimental data, with the ultimate strain at zero stress set between 2 and 10 times the strain related to the peak tensile strength.

Cracking behaviour has been modelled using a smeared crack approach with a rotated crack model [11,73]. Concrete properties have been derived from the experimental data or from [9] if necessary. Reinforcement has been modelled with a bilinear constitutive relationship with hardening law, capturing steel behaviour in both compression and tension. Properties were based on the experimental findings, with the Young's modulus equal to 210000 MPa and an ultimate strain of 9% [29]. The reinforcement has been represented using smeared and discrete approaches for the different types of rebars, following details described in [46–49].

3.3. Experimental and numerical results

As for both the RC *slender* and *non-slender members*, the NLNAs mirrored the experimental loading ones, starting with dead load and then, incrementally applying experimental actions until failure. Load step size has been chosen to balance accuracy and computational effort [12].

Tables 3 and 4 present a summary of the results, considering both the experimentally observed structural resistance (R_{Exp}) and corresponding values obtained through NLNAs ($R_{NLNA}(f_{Exp},a_{Exp})$).

These results are detailed alongside key structural parameters characterizing the structural response and primary features of the most likely failure mechanisms. With reference to both the RC *slender* and *non-slender members*, the NLN simulations have been able to reflect the experimentally observed failure mechanisms as demonstrated in [29,51] comparing the tests and numerical results. In detail, with reference to the RC *slender members,* the NLNAs have been able to catch the structural response for low (i.e., $\lambda < 75$) and high slenderness (i.e., $\lambda \geq 75$) values [29]. For low slenderness values, the failure mode involved a progressive increase in lateral displacement until the column lost equilibrium, accompanied by concrete failure in the compression zone and elastic tensile reinforcement. Conversely, for high slenderness values, loss of equilibrium occurred in the presence of lateral displacement, with both concrete and reinforcement within the elastic field. Regarding the RC *non-slender members*, as highlighted in the discussion provided by [51], the NLN models have successfully captured the load versus displacement

Table 3
Experimental (R_{Exp}) and numerical results $R_{NLNA}(f_{Exp};a_{Exp})$ for the 40 RC *slender members* [37–45].

Ref.	Exp. test	Type	λ [-]	*Structural resistance*	
				R_{Exp} [kN]	R_{NLNA} (f_{Exp},a_{Exp}) [kN]
[37]	2L20-30	*B*	15	750.0	694.3
	2L20-60			700.0	736.4
	2L8-120R			1092.0	1152.7
	4L8-30			1100.0	1032.9
	4L20-120			900.0	830.7
	4L8-120R			1247.0	1319.5
[38]	C000	*A*	17	559.6	560.6
	C020	*B*		327.3	328.5
	B020		52	271.5	263.7
	RL300		56	474.3	423.3
[39]	A-17-0.25	*B*	48	1181.4	1367.4
	C-31.7-0.25		94	333.4	280.1
[40]	3.3	*B*	59	782.6	856.4
	5.1			735.5	810.8
	4.1		88	367.7	391.7
[41]	N30-10.5-C0-3-30	*C*	21	16.6 (280)*1	16.6 (280)*1
	H60-10.5-C0-1-30			17.2 (412)*1	17.9 (412)*1
[42]	III	*A*	74	343.2	347.3
	Va			684.5	680.7
	2		83	235.4	762.0
	I		104	264.8	258.0
	VI		106	392.3	363.2
	15		136	549.2	560.3
	3		137	666.9	563.4
	8		83	235.4	236.8
	9	*B*	135	205.9	205.9
	12			112.8	112.2
	6		137	225.6	227.6
[43]	24D-2	*D*	104	198.4	192.8
	15E-2	*A*	139	161.0	129.3
[44]	S28	*B*	167	44.0	49.9
	S30			48.0	53.4
	S25		200	36.0	42.3
[45]	5	*A*	208	72.7	78.7
	6			72.2	82.3
	17 A		225	31.9	37.1
	20		243	37.9	39.8
	18			33.9	39.8
	8		274	31.9	31.0
	7			29.9	32.3

(-)*1: constant value of the axial load applied to the column during the experimental test.

Table 4
Experimental tests (R_{Exp}) and numerical results $R_{NLNA}(f_{Exp};a_{Exp})$ for the 16 RC *non-slender members* [46–49,51].

Ref.	Exp. test	$\varepsilon^{*1}_{s,max}$ [-]	*Structural resistance*	
			R_{Exp} [kN]	R_{NLNA} (f_{Exp} , a_{Exp}) [kN]
[46]	WT2	$4.05\bullet10^{-3}$	1085.1	1010.0
	WT3	$1.69\bullet10^{-3}$	884.0	980.0
	WT4	$5.62\bullet10^{-3}$	1670.0	1590.0
	WT6	$2.01\bullet10^{-2}$	989.5	1020.0
	WT7	$6.50\bullet10^{-3}$	1151.0	1180.0
[47]	B2.0A-4	$1.27\bullet10^{-2}$	1800.0	1840.0
	B3.0A-4	$1.00\bullet10^{-2}$	1400.0	1280.0
	B2.01	$5.41\bullet10^{-3}$	1590.0	1470.0
	B3.01	$6.55\bullet10^{-3}$	1020.0	1010.0
	B2.03	$4.34\bullet10^{-3}$	1400.0	1460.0
[48]	MB1ae	$2.69\bullet10^{-3}$	407.0	360.0
	MB1ee	$2.50\bullet10^{-3}$	413.0	305.0
	MB1ee1	$7.18\bullet10^{-3}$	416.0	405.0
	MB4ee	$7.88\bullet10^{-3}$	400.0	370.0
	MB1aa	$2.33\bullet10^{-3}$	350.0	325.0
[49]	SW11	$1.53\bullet10^{-2}$	252.6	222.5

(-)^{*1}: maximum strain attained in the primary reinforcement in NLNA conducted with experimental material and geometrical properties.

curves, as well as have been able to identify both the region with concrete failure in compression and associated global mechanism.

Table 3 reports the results for the RC columns, categorizing them with respect to their slenderness values (λ), in accordance with [50]. The slenderness value λ effectively measures the growing influence of geometrical non-linearities when compared to material ones, as suggested in [29]. In this study, λ is used to present the results pertinent to the RC *slender members*.

Table 4 lists the results, using the maximum strain in the so-called "primary reinforcement" ($\varepsilon_{s,max}$), as the key structural parameter. This maximum strain is obtained from the NLNAs with experimental values for both material properties (f_{Exp}) and geometrical characteristics (a_{Exp}). As defined in [51], the primary reinforcement identifies the elements primarily involved in the resistance mechanism, essential for maintaining equilibrium immediately prior to failure. This parameter, $\varepsilon_{s,max}$, accounts for the nature of the RC system failure mode, distinguishing between ductile and brittle mechanisms [51]. In this study, $\varepsilon_{s,max}$ will be employed to discuss the findings of the RC *non-slender members* together with its normalized value with respect to the yielding strain ε_y (i.e., $\varepsilon_{s,max}/\varepsilon_y$).

Fig. 2(a)-(b) depicts two distinct scatter plots that show the comparison in terms of global structural resistance between the experimental results (R_{Exp}) and corresponding numerical values (R_{NLNA}), which are computed using experimental material properties (f_{Exp}) and geometrical properties (a_{Exp}) for both the RC *slender* and *non-slender members*. These calculations are based on the set of modelling assumptions outlined in Tables 1 and 2.

To evaluate the validity of the chosen modelling assumptions, the observed value of the model uncertainty random variable $\vartheta_{obs}=R_{Exp}/R_{NLNA}(f_{Exp},a_{Exp})$ has been determined for each RC member [50,55,57,56]. Statistical analysis of the ratio ϑ_{obs} has been performed using the Maximum Likelyhood (ML) method [74] with the assumption of lognormally distributed variable [50,55,57,56]. The results of the statistical analysis are reported in Fig. 2(a)-(b) in terms of mean value $\mu_{\vartheta,obs}$ and CoV $V_{\vartheta,obs}$ (being $\sigma_{\vartheta,obs}$ the related standard deviation) [50].

As for the RC *slender members*, it is observed that the data tend to follow the line related to un-biased model (i.e., black dashed line). This is also indicated by the ML estimates related to lognormal distribution, with a mean value $\mu_{\vartheta,obs}$= 0.99 (i.e., closely un-biased model) and CoV $V_{\vartheta,obs}$= 0.10.

Fig. 2(b) shows the same analysis for the 16 RC *non-slender members* [46–49]. The mean value is slightly higher and equal to $\mu_{\vartheta,obs}$= 1.05, while the CoV is equal to $V_{\vartheta,obs}$= 0.09. Similarly, most of the data is close to the un-biased with a slightly lower dispersion compared to Fig. 2(a).

In both cases, the charts and statistical analyses suggest that the distribution of the experimental results is close to the predicted theoretical values, indicating that the NLN models and related modelling assumptions are adequate for describing the behaviour of the herein considered RC members.

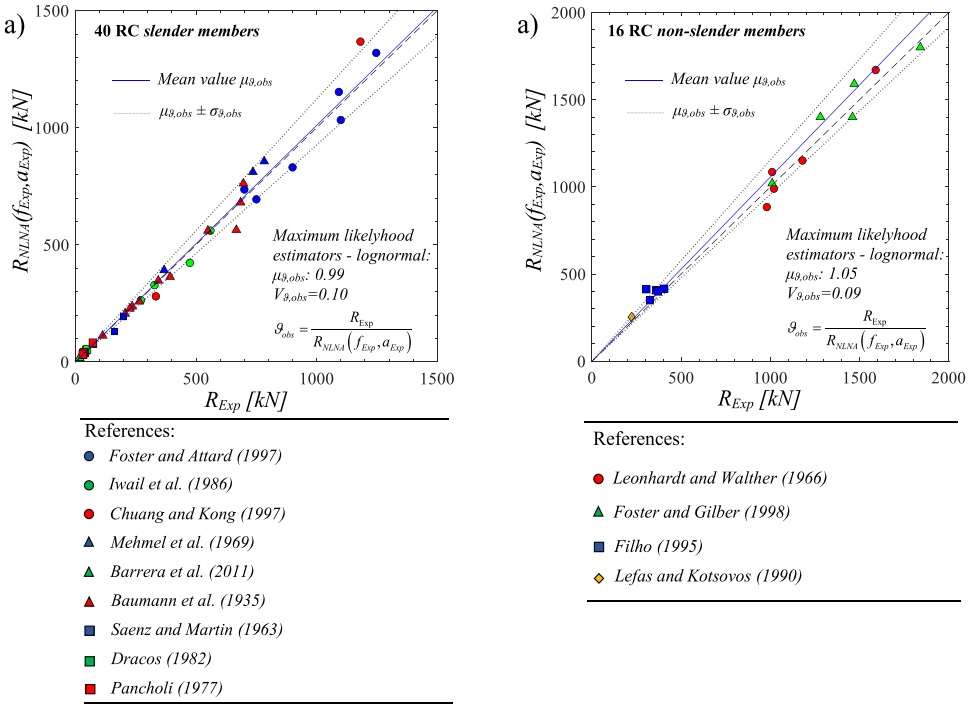

Fig. 2. Comparison between the experimental (R_{Exp}) and NLN results ($R_{NLNA}(f_{Exp}, a_{Exp})$) for the 40 RC *slender members* [37–45,50] (a) and 16 RC *non-slender members* [46–49,51] (b).

Note that these results are used to justify the modelling assumptions adopted herein, and combined with literature studies [50,55,56] to compute the statistics related to the epistemic uncertainties in the extensive probabilistic analysis proposed in the following sections.

Also grounding on [50,55,57,56], the so far adopted modelling assumptions can be considered suitable to be adopted for a comprehensive probabilistic investigation of structural resistance of the RC *slender* and *non-slender* members including both aleatory and epistemic uncertainties.

Next section will be focused on the probabilistic analysis of the global structural resistance for the 56 RC members.

4. Probabilistic analyses to assess the resistance random variables

This section describes the probabilistic analysis of the global structural resistance of the 40 RC *slender* [37–45] and 16 RC *non-slender members* [46–49] including both aleatory (i.e., materials and geometry) and epistemic (i.e., model) uncertainties. Initially, the assumptions underlying the probabilistic models for the associated random variables are introduced. Subsequently, the resistance random variables considered are defined. Lastly, a discussion of the sensitivity of the global structural response to both aleatory and epistemic uncertainties is undertaken.

4.1. Hypotheses for probabilistic modelling of both aleatory and epistemic uncertainties

The NLN models have been used to carry out a probabilistic assessment concerning the global structural resistance of both the 40 RC *slender* and 16 RC *non-slender members*. In this subsection, the hypotheses for probabilistic modelling of both aleatory (i.e., materials and geometry) and epistemic (i.e., model) uncertainties random variables are introduced according to [10,52]. In Tables 5–6, the probabilistic models applied to the involved random variables are listed. These models respect the principles outlined in [52], also applied by [14,29,50,55,56].

Table 5 presents the hypotheses for probabilistic modelling of aleatory uncertainties in both the 40 RC *slender members* [37–45] and 16 RC *non-slender members* [46–49]. It focuses on the various random variables associated with materials and geometrical properties according to [10, 14,29,52]. Note that the mean value of the different random variables is assumed as the related experimental one when available from the original studies. Specifically, the concrete cylinder compressive strength (f_c) follows a lognormal distribution with a mean value $f_{c,Exp}$ and a CoV (V_c) of 0.15, in accordance with [10]. The reinforcement tensile yielding strength (f_y) and ultimate tensile strength (f_u) also follow a lognormal distribution, with mean values of $f_{y,exp}$ and $f_{u,exp}$, respectively, and a CoV of 0.05. It is noted that if the experimental value $f_{u,Exp}$ is unavailable, the mean ultimate tensile strength is determined by assuming a 15% increase over the experimental tensile yielding strength $f_{y,Exp}$. The reinforcement Young's modulus (E_s) has a mean of 210000 MPa with a CoV of 0.03. The reinforcement ultimate strain in elongation (ε_u) has a mean of 0.075 with a CoV of 0.09. Statistical correlations of both f_y and f_u with ε_u are considered in line to [52] as reported in Table 5. In terms of geometrical properties, the concrete cover (C) deviation follows a normal distribution with a mean of 0 mm and a standard deviation of 5 mm. The deviation of cross-sections and structural members size (s) is also normally distributed with a mean value of $0\ mm \leq 0.003\ s_{Exp} \leq 3\ mm$ and a standard deviation of $4 + 0.006\ s_{Exp} \leq 10\ mm$. Lastly, the axial load eccentricity (e) for the RC *slender members* is normally distributed around e_{Exp} with a standard deviation of $L_{Exp}/1000$.

Table 6 outlines the hypotheses for probabilistic modelling of the epistemic uncertainties in both the 40 RC *slender members* [37–45] and 16 RC *non-slender members* [46–49]. It focuses on the model uncertainty random variable (ϑ) for both categories of members. In both the cases, the selected statistical parameters for ϑ are derived from [50,55,56] to avoid their underestimation and include the influence of both the "within" and "between" model uncertainties [56] and relate to the

Table 6
Hypotheses for probabilistic modelling of epistemic uncertainties in both the 40 RC *slender members* [37–45] and 16 RC *non-slender members* [46–49].

Random variable (Epistemic)	Probabilistic distribution	Mean value μ_ϑ [-]	CoV V_ϑ [-]	Ref.
Slender members				
Model uncertainty[*1] ϑ	*Lognormal*	1.04	0.15	*Approach A* of [50]
Non-slender members				
Model uncertainty[*2] ϑ	*Lognormal*	1.03	0.12	[55,56]

[*1] (-) "Pure" value of the model uncertainty [50,56] assuming a significant effect of the experimental uncertainties in line to [50].
[*2] (-) "Pure" value of the model uncertainty [50,56] assuming a limited effect of the experimental uncertainties in line to [50].

Table 5
Hypotheses for probabilistic modelling of aleatory uncertainties in both the 40 RC *slender members* [37–45] and 16 RC *non-slender members* [46–49].

Random variable (Aleatory)	Probabilistic distribution	Mean value	CoV [-]	Standard deviation	Statistical correlation	Ref.
Material properties						
Concrete cylinder compressive strength f_c [MPa]	*Lognormal*	$f_{c,Exp}$	0.15	-	-	[10, 52]
Reinforcement tensile yielding strength f_y [MPa]	*Lognormal*	$f_{y,Exp}$	0.05	-	f_u (0.85)[*2], ε_u(−0.50)[*2]	[52]
Reinforcement ultimate tensile strength f_u [MPa]	*Lognormal*	$f^{*1}_{u,Exp}$	0.05	-	f_y (0.85)[*2], ε_u(−0.55)[*2]	[52]
Reinforcement Young modulus E_s [MPa]	*Lognormal*	210000	0.03	-	-	[52]
Reinforcement ultimate strain in elongation ε_u [-]	*Lognormal*	0.075	0.09	-	f_y (−0.50)[*2], f_u (−0.55)[*2]	[52]
Geometrical properties						
Concrete cover (C) deviation $Yc=C-C_{exp}$ [mm]	*Normal*	0	-	*5*	-	[52]
Deviation of the cross-sections and structural members size (s)[*3] $Y_s=s-s_{Exp}$ [mm]	*Normal*	$0 \leq 0.003 s_{Exp} \leq 3$	-	$4 + 0.006\ s_{Exp} \leq 10$	-	[52]
Axial load eccentricity (*slender members*) e [mm]	*Normal*	e_{Exp}	-	$L_{Exp}/1000$	-	[52]

[*1] In cases where the experimental value $f_{u,Exp}$ is unavailable, the mean ultimate tensile strength is determined by assuming a 15% increase over the experimental tensile yielding strength $f_{y,Exp}$.
* 2 (-) Correlation coefficient in relation to another material parameter.
[*3] (-) The size of structural members (s) denotes the base (b), height (h) of cross-sections and length (L) of main body for the RC *slender members* and the main dimensions for the *non-slender members* (i.e., width, height and thickness).

"pure" or "actual" value of model uncertainty (i.e., deprived of the epistemic uncertainty related to experimental deviations and measurements errors) [50,56]. For the RC *slender members*, the model uncertainty is assumed to follow a lognormal distribution with a mean value of 1.04 and a CoV of 0.15, according to [50]. The "pure" value of model uncertainty is derived assuming a significant influence of the experimental uncertainty in line with the *Approach A* of [50]. This assumption is justified by the complexity related to realization of tests on RC members with high slenderness [50]. Similarly, for the RC *non-slender members*, the model uncertainty is assumed to follow a lognormal distribution with a mean value of 1.03 and a CoV of 0.12, according to [55,56]. The extensive data from [55,56] has been used to characterise the statistical uncertainty within the probabilistic analyses presented in the next. This is also the pure value of the model uncertainty, considering a limited effect of the experimental uncertainties as typically happen in case of tests of non-corroded RC members [64] and according to [50,55,56]. Note that the data summarized in Table 6 reflects the model uncertainties related to structural configurations similar to ones investigated in this study and by [50,55,56].

This set of probabilistic hypotheses, for the main involved material, geometrical and model uncertainties, are useful to characterize the resistance random variables discussed in next subsections.

4.2. Characterization of the global resistance random variables

The global resistance random variables (GRRVs) have been herein treated in accordance with Eq.(1) [54]. The probabilistic analysis of the GRRVs has been performed by adopting the latin hypercube sampling (LHS) method [75] to sample two groups of 100 realizations. The first group involves only the aleatory (i.e., materials and geometrical) uncertainties. Instead, the second group includes both the aleatory and epistemic (i.e., model uncertainty) random variables.

Consequently, two groups of 100 NLN sampled models [29] have been defined for each of both the 40 RC *slender members* [37–45] and 16 RC *non-slender members* [46–49] leading to the evaluation of two distinct GRRVs through Eq.(9) and Eq.(10), derived from Eq.(1) according to [54], respectively:

$$R = R_{NLNA}(f,a) \text{ sampling from } \textit{only aleatory uncertainties} \tag{9}$$

$$R_{Gl} = \vartheta \cdot R_{NLNA}(f,a) \text{ sampling from } \textit{both aleatory and epistemic uncertainties} \tag{10}$$

Specifically, the first GRRV, denoted as R, comprises 100 NLN sampled models corresponding to only the randomness in materials (f) and geometrical (a) properties (i.e., aleatory), in line with Table 5. In contrast, the second GRRV, denoted as R_{Gl}, has been assessed through another group of 100 NLN sampled models, which consider both aleatory uncertainties and epistemic (i.e., model (ϑ)) uncertainties, as defined in Tables 5 and 6. These two groups of sampled models, characterizing the GRRVs R and R_{Gl}, have been employed to examine the impact of both aleatory and epistemic uncertainties on the global nonlinear response of both *slender* and *non-slender* members.

In Annex A, Figures A1-A3 present, for each one of both the 40 RC *slender members* [37–45] (Figure A1) and 16 RC *non-slender members* [46–49] (Figures A2-A3), the 'empirical' and 'theoretical' cumulative density functions (CDFs) related to the two GRRVs (i.e., R and R_{Gl}). These representations show the influence of both aleatory and epistemic uncertainties on the global structural response and difference between R and R_{Gl}. The Anderson-Darling statistical tests [76] have been performed on the probabilistic results for both R and R_{Gl}, to determine whether the obtained results follow a lognormal distribution (i.e., the null hypothesis). The latter, implying a lognormal distribution for both R and R_{Gl}, has been examined and accepted at a 5% significance level for each group of the sampled NLN models, as testified by the 'P-values' in Figures A1-A3. The statistical parameters of the 'theoretical' lognormal CDFs have been estimated using the ML method [77,78], through the ML estimators. The statistical parameters for the GRRV R have been adopted to determine the related mean value (μ_R), bias factor (δ_R) and CoV (V_R) considering only the influence of the aleatory uncertainties. Similarly, the statistical parameters for the GRRV R_{Gl} have been used to assess the mean value (μ_{Gl}), bias factor (δ_{Gl}) and CoV (V_{Gl}) considering the contribution of both aleatory and epistemic uncertainties. As for the statistics related to the epistemic uncertainties, the results from literature [50,55,56] are employed (Section 4.1).

In Fig. 3(a)-(b) and Fig. 4(a)-(b), the values of δ_R and V_R are depicted for both the 40 RC *slender* [37–45] and 16 RC *non-slender members* [46–49], respectively. As for the 40 RC *slender members*, the δ_R values, on average, fall below 1 and are approximately around 0.9. Conversely, for the 16 RC *non-slender members*, these values tend to 1 in most cases. This situation reflects the achievements of [29] and [51]. Concerning the 40 RC *slender members,* Fig. 3(b) shows that, due to the growing influence of geometrical uncertainty affecting the geometrically non-linear behaviour for growing slenderness, the V_R value increases approximatively linearly with λ. This is evidence of the fact that V_R is significantly affected by the nature of the failure mechanism.

As for the 16 RC *non-slender members*, Fig. 4(b) depicts a progressive decreasing of the value of V_R as a function of $\varepsilon_{s,max}$ normalized with respect to the primary reinforcement yielding strain ε_y. These results reflect the fact that when the values of $\varepsilon_{s,max}/\varepsilon_y$ increases, it leads to a greater influence of random variability in the properties of the reinforcement compared to those of concrete in the global failure mechanism [51]. Then, progressive more ductile failure mechanisms lead to a decreasing value of V_R. Conversely, when $\varepsilon_{s,max}/\varepsilon_y$ values are close to or lower than 1, the influence of concrete properties becomes more significant due to more brittle failure mechanisms for concrete failure. Additionally, comparing the findings in Fig. 4(b) with those provided by [51] for the 16 RC *non-slender members* solely considering the influence of material uncertainties, it becomes evident that, on average, the effect of geometrical uncertainties has a relatively lower impact on the V_R value when compared to materials uncertainties (i.e., approximately 10%).

Fig. 3(e)-(f) and Fig. 4(e)-(f) report the values of δ_{Gl} and V_{Gl} for both the 40 RC *slender* [37–45] and 16 RC *non-slender members* [46–49], respectively. The values of δ_{Gl} and V_{Gl} include the additional variability related to the epistemic uncertainty and follow the general trend as discussed for δ_R and V_R. In detail, an increase of the average value of δ_{Gl} with respect to δ_R can be appreciated leading to the bias factor closer to unit when epistemic uncertainty is also included in the analysis. As expected, the V_{Gl} values are higher than V_R.

Finally, Fig. 3(c)-(d) and Fig. 4(c)-(d) illustrate the values of both δ_{Gl}^{II} and V_{Gl}^{II} useful to implement *Approach II* to evaluate the global safety factors. In particular, the values have been evaluated by means of Eq.s (7)-(8) including both aleatory and epistemic uncertainties. Fig. 3(c)-(d) and Fig. 4(c)-(d) show a good agreement with the data in Fig. 3(e)-(f) and Fig. 4(e)-(f).

In next subsection, the sensitivity of the global structural response with respect to both aleatory and epistemic uncertainties is discussed.

4.3. Sensitivity of the global structural response

The sensitivity of the global structural resistance, represented by the GRRV R_{Gl}, with respect to both aleatory and epistemic uncertainties is discussed considering both the 40 RC *slender members* [37–45] and 16 RC *non-slender members* [46–49]. Fig. 5(a)-(b) and Fig. 6(a)-(b), for the two families of RC members, illustrate, respectively, the ratio between the V_R values (associated to aleatory uncertainties only) and V_ϑ values (related to model uncertainty only) with respect to the CoV V_{Gl} (estimated including both aleatory and epistemic uncertainties).

Considering the 40 RC *slender members*, Fig. 5(a)-(b) illustrates that the significance of the aleatory uncertainties in affecting the variability of the global structural response increases for higher values of the

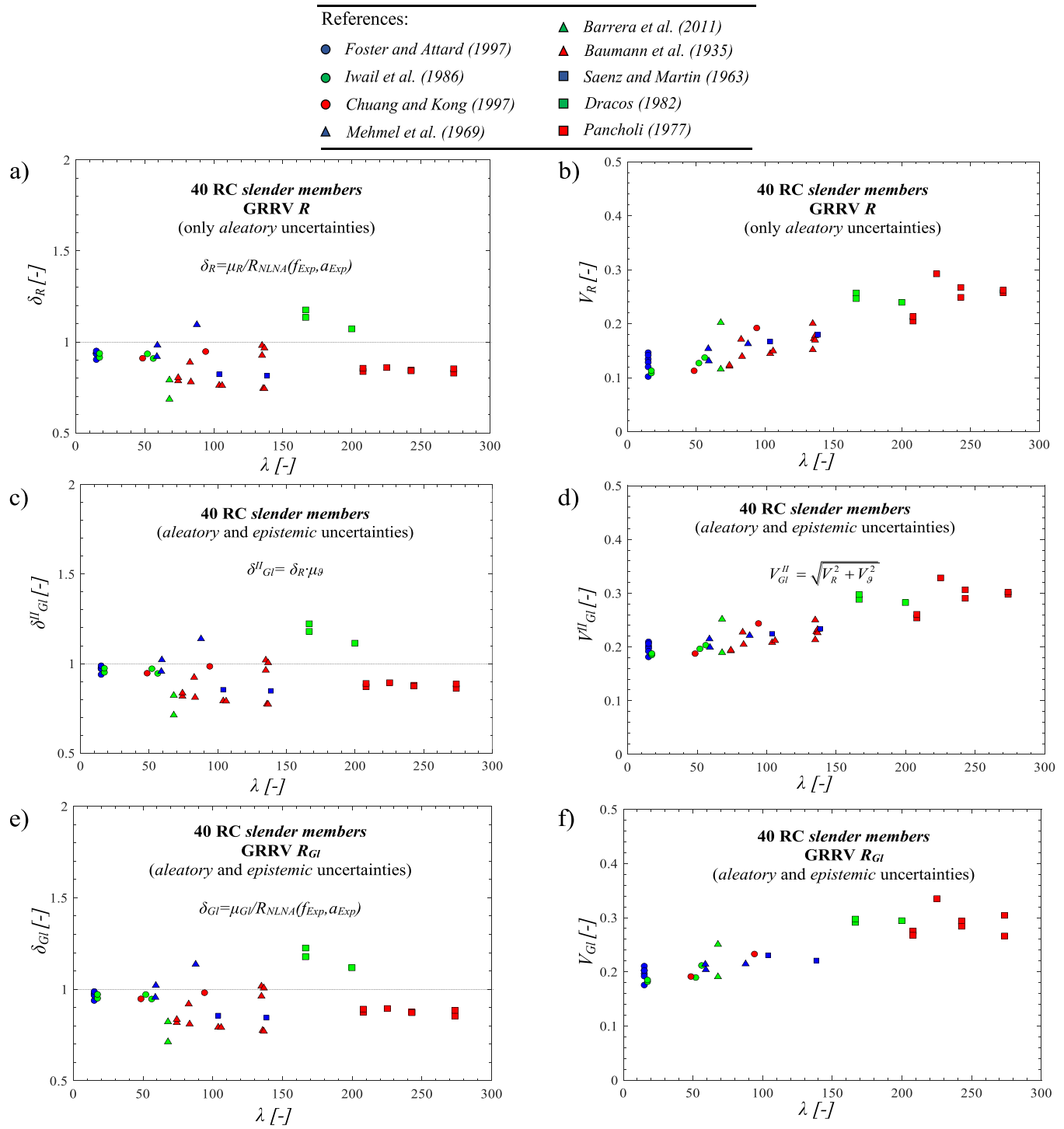

Fig. 3. 40 RC *slender members* [37–45]: bias factors δ_R and δ_{Gl} with respect to GRRVs R and R_{Gl} (a),(e), respectively, and δ_R^{II} according to approximation of *Approach II* (c); CoV values V_R and V_{Gl} (b),(f) with respect to GRRVs R and R_{Gl}, respectively, and V_R^{II} according to approximation of *Approach II* (d).

slenderness (λ). Conversely, the influence of the epistemic uncertainties decreases under the same conditions. In fact, due to the increasing relevance of the geometrical non-linearity related to structural behaviour, the aleatory uncertainties (especially, the geometrical ones) mainly affect the CoV V_{Gl}. This result is furtherly highlighted in Fig. 5(c) showing that the ratio between V_R and V_ϑ is lower than one for slenderness values lower than around 75. For high slenderness values, the aleatory uncertainties (especially geometrical ones) dominate the variability of the global structural resistance. On the contrary, for low values of λ, the epistemic uncertainty dominates with respect to the aleatory ones. It is also worth mentioning that, in accordance with [29], for λ values lower than 75, the material uncertainties have a greater influence on V_R compared to geometrical uncertainties.

With reference to the 16 RC *non-slender members*, Fig. 6(a)-(b) shows that the epistemic uncertainty (i.e., model) prevails the aleatory ones in almost all the situations moving from brittle to ductile failure modes. This result agrees with the ones achieved for the case of the *slender members* characterized by low slenderness values. In fact, Fig. 6(a)-(b) highlights that the bigger is the ratio $\varepsilon_{s,max}/\varepsilon_y$, the more ductile is the response of the structural system, the lower is the value of V_R and, for

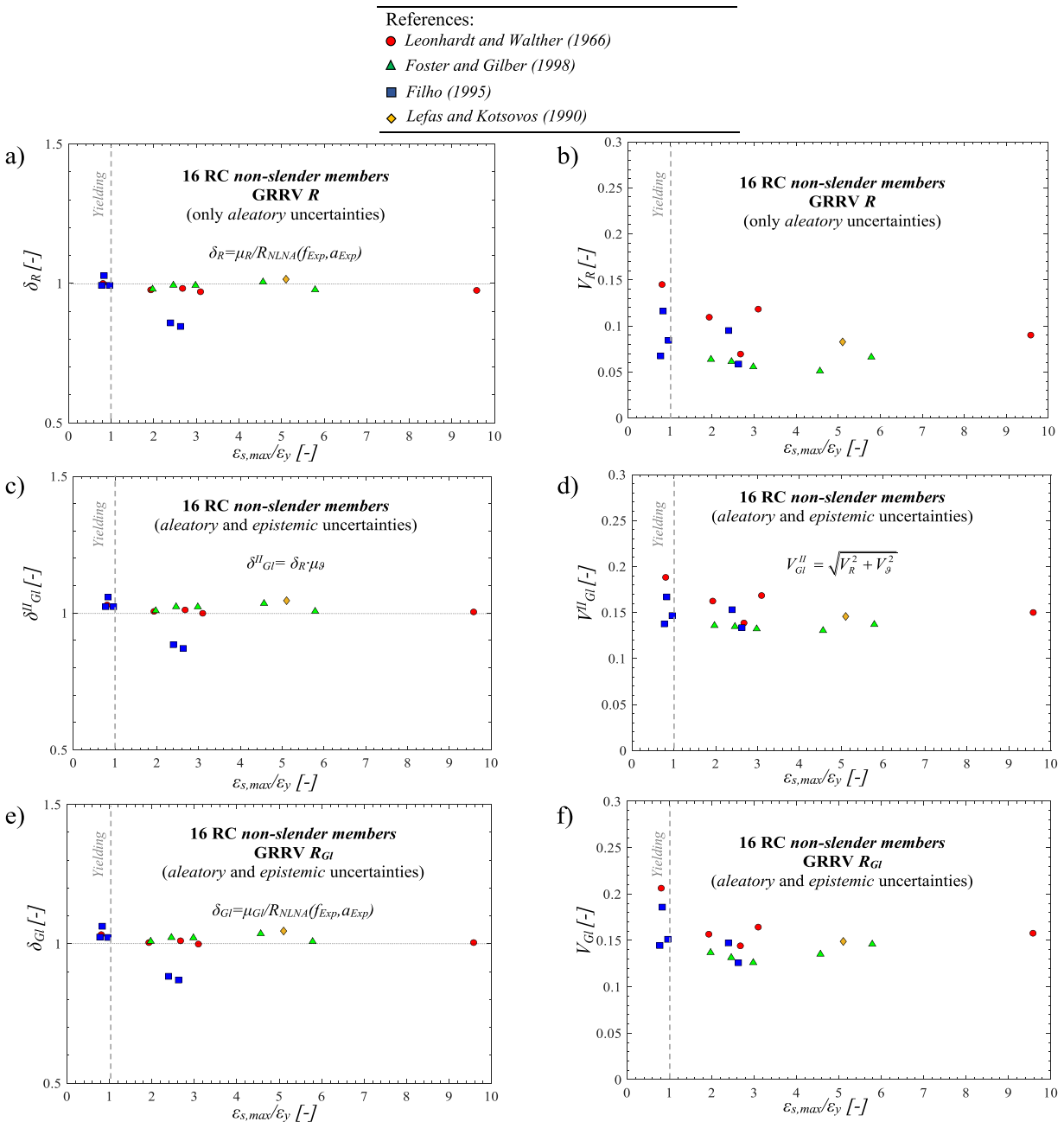

Fig. 4. 16 RC *non-slender members* [46–49]: bias factors δ_R and δ_{Gl} with respect to GRRVs R and R_{Gl} (a),(e), respectively, and δ_R^{II} according to approximation of *Approach II* (c); CoV values V_R and V_{Gl} (b),(f) with respect to GRRVs R and R_{Gl}, respectively, and V_R^{II} according to approximation of *Approach II* (d).

instance, the bigger is the influence of the epistemic uncertainty on V_{Gl}. Specifically, Fig. 6(a)-(b) emphasizes that as the ratio $\varepsilon_{s,max}/\varepsilon_y$ increases, the structural system response becomes more ductile with lower V_R values. Additionally, it underscores that a larger $\varepsilon_{s,max}/\varepsilon_y$ ratio corresponds to a greater influence of the epistemic uncertainty on V_{Gl}. This result is furtherly clarified in Fig. 6(c): the ratio between V_R and V_ϑ for the 16 RC *non-slender members* falls below unit for a major part of the cases, becoming higher than or close to 1.00 only for more brittle failure mechanisms, significantly affected by random variability of concrete cylinder compressive strength (represented by its CoV V_c). This result demonstrates that, under the assumptions presented in this paper, the model uncertainty related to NLNAs can be dominant with respect to aleatory ones. This seems to be in opposition with respect to the assumptions performed by codes [10] in relation to application of the GRM. However, this result should be furtherly discussed in terms of achieved target level of reliability investigating and comparing the values of the global safety factors assessed through *Approach I*, *II* and *III*. It is important to underline that, the latter considerations depend on the probabilistic modelling hypotheses. In fact, [51] demonstrates that for different values of the concrete cylinder compressive strength (V_c), as for existing RC structures, the ratios presented in Figs. 5–6 can differ, leading to different conclusions about the dominance or non-dominance of the specific resistance variable.

Note that the assumptions on the model uncertainties in Table 6 refer to specific studies [50,56] as well as the assumptions of Section 3 are frequently accepted for calibration of design codes [9,10]. Moreover, the epistemic uncertainty needs to be further assessed since software advancements.

The following section aims to estimate the global safety factors as a function of both uncertainties.

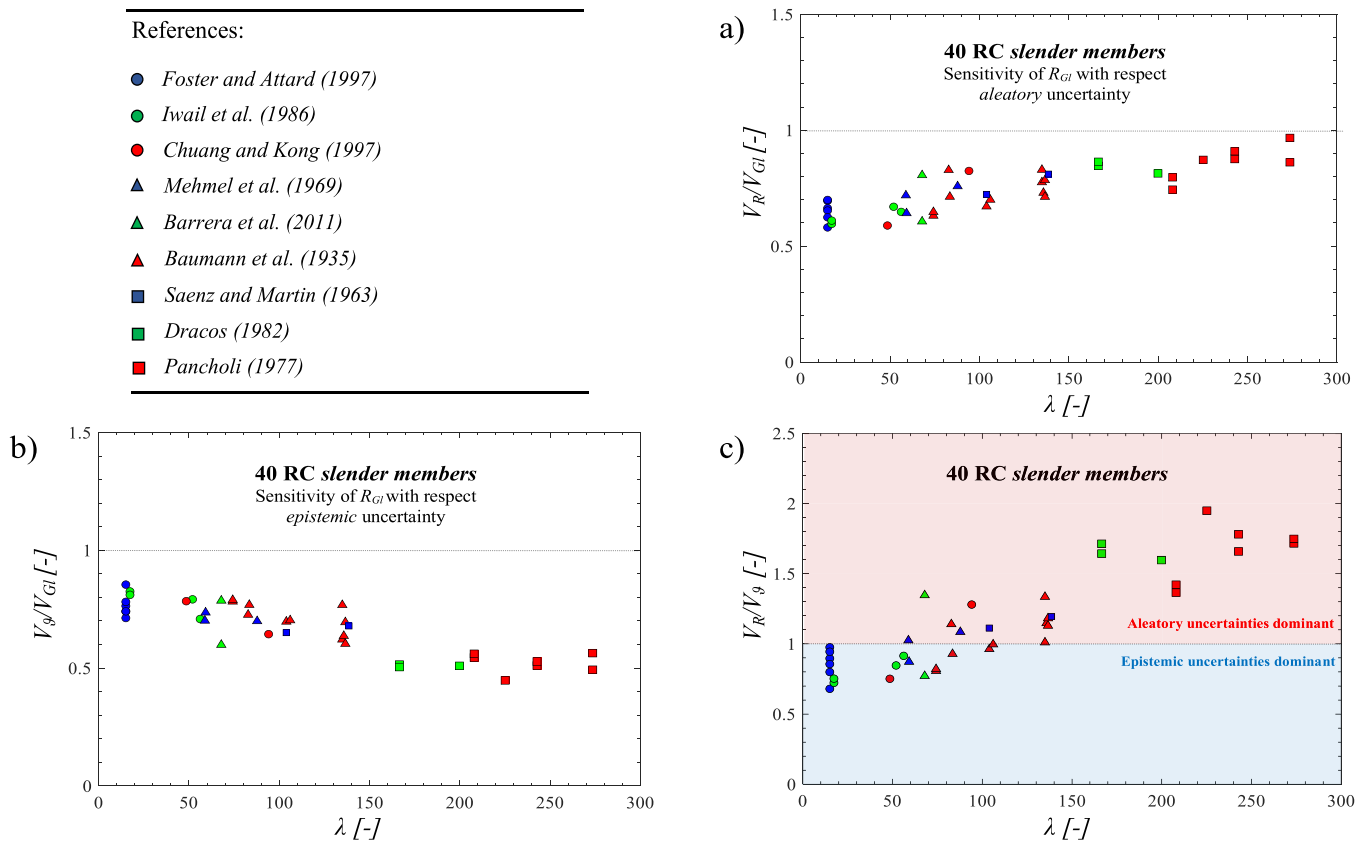

Fig. 5. 40 RC *slender members* [37–45]: sensitivity of global structural resistance with respect to aleatory (a) and epistemic uncertainties (b); comparison between CoV values related to aleatory and epistemic uncertainties (c).

5. Comparison and discussion of the approaches to estimate the global safety factors

This section deals with the approaches conceived to estimate the global safety factor (γ_{Gl}), as outlined in Section 2. Specifically, the comparison is conducted using the results obtained from the probabilistic characterization of the GRRVs R and R_{Gl}, described in Section 4. In detail, this section compares *Approach I* and *Approach II* with respect to *Approach III*, which is regarded as the reference method since incorporates both aleatory and epistemic uncertainties in the probabilistic analysis. As demonstrated in Section 4, the assumption that aleatory uncertainties dominate over epistemic ones is not always accurate within safety assessments using NLNAs. *Approach I* usually adopts the former assumption [10–14,56]. However, for the sake of a comprehensive evaluation, *Approach I/b* is herein introduced as a modification of *Approach I* assuming that epistemic uncertainties (i.e., model) dominate over aleatory ones. This is achieved by employing appropriate FORM factors α_R and α'_R to calculate γ_R and γ_{Rd} [10]. The comparison between the global safety factors is carried out for a consistent target reliability level. Specifically, when evaluating newly realized RC structures with a reference period of 50 years, the target reliability index is commonly set at $\beta_t = 3.8$ [10,28,31] in case of normal class in terms of consequences of structural failure. In the case of existing structures or different design assumptions, it is recommended to consult [32] to ascertain the most appropriate target reliability index as a function of different reference periods and costs for safety measures.

The comparison between the different approaches to evaluate the global safety factors, for both the 40 RC *slender members* [37–45] and 16 RC *non-slender members* [46–49], is proposed in Figs. 7 and 8. Specifically, Fig. 7(a),(c),(e),(g) and Fig. 8(a),(c),(e),(g) depict the values of the global safety factors following *Approach I*, *I/b*, *II* and *III*, respectively. Meanwhile, Fig. 7(b),(d),(f) and Fig. 8(b),(d),(f) compare *Approach I*, *I/b* and *II* with *Approach III* by presenting the ratios between the obtained values of the global safety factors together with both the moving mean (the black dashed line) and CoV (the grey continuous line) values. Detailed information regarding the calculated global safety factors for the various approaches for both the *slender* and *non-slender members*, along with the design values of the global structural resistance (R_d) determined using Eq.(2), can be found in Table B1 and Table B2 of Annex B.

In the following, the discussion of the comparison between the approaches is outlined for both the 40 *RC slender member* and 16 RC *non-slender members*. After that, general comments are provided.

Concerning the 40 *RC slender members*, *Approach I* leads to ratios $\gamma^{I}_{Gl}/\gamma_{Gl}$ (Fig. 7(b)) that vary between values from around 0.95 for slow slenderness values to 1.06 for high slenderness values. This implies that, as the slenderness increases and, for instance, the significance of aleatory uncertainties becomes more pronounced (Fig. 5), *Approach I* will consistently yield safer estimates of the global safety factor (γ^{I}_{Gl}) in comparison to the reference value (γ_{Gl}). This outcome is a result of the assumption of dominant aleatory uncertainties with respect to epistemic ones in *Approach I*. In general, *Approach I* leads to values close to 1.00 for low slenderness values and safer values for higher slenderness values, maintaining a relatively constant dispersion of the data, with the CoV ranging from 0.03 to 0.05. Fig. 7(d) presents a comparison between the global safety factors derived from *Approach I/b* and *Approach III* through the ratio $\gamma^{I/b}_{Gl}/\gamma_{Gl}$. In this case, where the dominant resistance variable is the model uncertainty (i.e., epistemic) over aleatory one, the trend is the opposite of the one in Fig. 7(b). Indeed, for low slenderness values, the values of $\gamma^{I/b}_{Gl}$ are safer compared to γ_{Gl}, with ratios close to 1.01. However, as the slenderness increases, *Approach I/b* leads to significantly less safe estimates of $\gamma^{I/b}_{Gl}$, approaching ratios of 0.88. In addition, the data dispersion increases notably for higher λ, ranging from 0.02 to 0.07. Fig. 7(f) shows the comparison between the global safety factors γ^{II}_{Gl} of

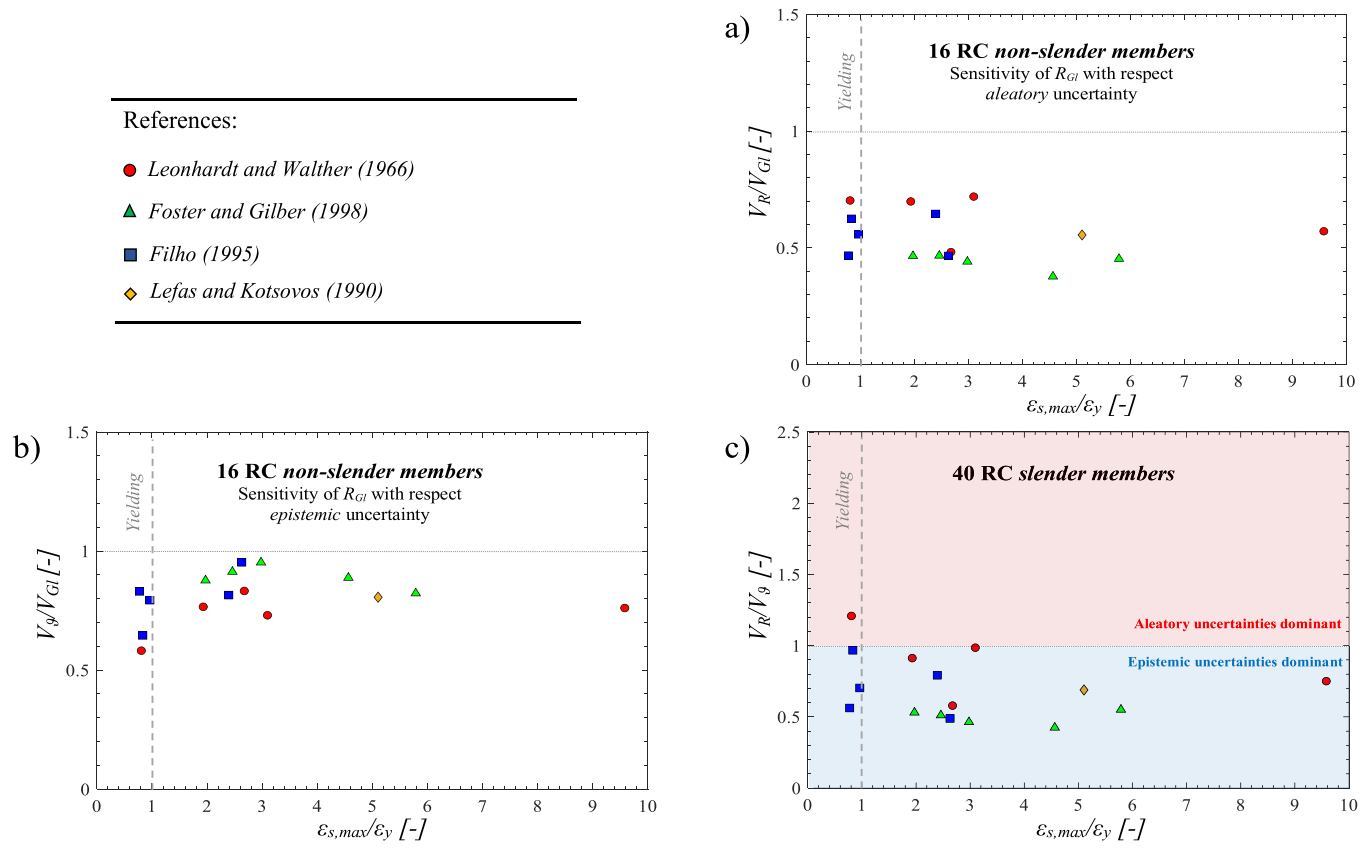

Fig. 6. 16 RC *non-slender members* [46–49]: sensitivity of global structural resistance with respect to aleatory (a) and epistemic uncertainties (b); comparison between the CoV values related to aleatory and epistemic uncertainties (c).

Approach II and *Approach III* for the 40 *RC slender member* in terms of ratios $\gamma_{Gl}^{II}/\gamma_{Gl}$. The latter results show that *Approach II* performs significantly better than both *Approach I* and *I/b*. In fact, the values of the ratio $\gamma_{Gl}^{II}/\gamma_{Gl}$ are constantly aligned around 1 for all the range of slenderness values having a scattering that moves from CoV of 0.02 to 0.04. This demonstrates that the adoption of a single global safety factor, without splitting the values for aleatory and epistemic uncertainties as for *Approach I* and *I/b*, has a more comprehensive consideration of the significance of various sources of uncertainty in estimating the global safety factor. It achieves this without implying safe or unsafe deviations, even when one type of uncertainty is significantly more dominant than the other one. Moreover, the approximation of Eq.s(7)-(8) implies an accurate estimation of the values of V_R^{II} and δ_R^{II} with respect to V_R and δ_R (Fig. 3) leading to global factors values γ_{Gl}^{II} of Fig. 7(e) very close to the ones (γ_{Gl}) in Fig. 7(g).

Regarding the 16 RC *non-slender members*, the results between *Approach I* and *Approach III* in terms of the ratio $\gamma_{Gl}^{I}/\gamma_{Gl}$ as a function of $\varepsilon_{s,max}/\varepsilon_y$ are presented in Fig. 8(b). These outcomes indicate that this ratio remains relatively stable at around 0.95, demonstrating a lower unsafe deviation of γ_{Gl}^{I} compared to γ_{Gl}. The dispersion of the results ranges from a CoV of approximately 0.02 to 0.05. Similarly to the 40 RC *slender members*, this outcome derives from the assumption of aleatory uncertainties dominating over epistemic ones that, as showed in Fig. 6, is not satisfied in particular for more ductile failure mechanisms for increasing ratio $\varepsilon_{s,max}/\varepsilon_y$.

Fig. 8(d) shows the comparison between the global safety factors derived from *Approach I/b* and *Approach III* through the ratio $\gamma_{Gl}^{I/b}/\gamma_{Gl}$. In this circumstance, the assumption of epistemic uncertainty dominating with respect to aleatory ones within *Approach I/b* leads to estimate $\gamma_{Gl}^{I/b}/\gamma_{Gl}$ close or quite higher than one (i.e., 1.02), with a quite constant safe deviation depending on $\varepsilon_{s,max}/\varepsilon_y$. In this case, the dispersion of the data of Fig. 8(d) moves from CoVs of 0.05 for low $\varepsilon_{s,max}/\varepsilon_y$ to values close to 0.01 for high $\varepsilon_{s,max}/\varepsilon_y$. Finally, Fig. 8(f) shows the comparison between *Approach II* and *Approach III* for the 16 RC *non-slender members*. Once more, *Approach II* appears to outperform both *Approach I* and *I/b* when estimating γ_{Gl}^{II} compared to γ_{Gl}. In fact, the ratio $\gamma_{Gl}^{II}/\gamma_{Gl}$ remains relatively constant at around 1.00 for both brittle (low $\varepsilon_{s,max}/\varepsilon_y$) and ductile (high $\varepsilon_{s,max}/\varepsilon_y$) failure mechanisms, with a dispersion ranging from 0.03 to values below 0.01. In fact, the results in terms of global safety factors presented in Fig. 8(e) for *Approach II* are very similar to the ones in Fig. 8 (f) for *Approach III*.

The results mentioned above indicate that adopting *Approach I* instead of *Approach I/b* can lead to situations, especially for slender systems, where the estimation of the global safety factor (γ_{Gl}) is sometimes on the safe side, implying hidden safety [79] in the estimation of the design value of global structural resistance through Eq.(2). However, in some situations, it may lead to estimation of γ_{Gl} on the unsafe side, implying some hidden lack of safety (i.e., "hidden un-safety") within the reliability assessment through the GRM. The balance between these two situations is influenced by the assumptions related to the variability of both aleatory and epistemic uncertainties and can vary from case to case. In fact, especially for non-slender systems, *Approach I/b* leads to results on the safe side. This makes the adoption of *Approach I* or *Approach I/b* dependent on the assumption between the source of uncertainty that dominates the response in terms of global structural resistance.

Approach II leads to accurate estimations of the global safety factors in comparison to *Approach III*, regardless of the significance of aleatory or epistemic uncertainties. This finding holds true for both the 40 RC *slender members* and 16 RC *non-slender members* and suggests for its general validity with independence on the nature of the failure mechanism.

For instance, *Approach II* can be considered as a very accurate methodology to assess the global safety factor within the GRM using Eq.

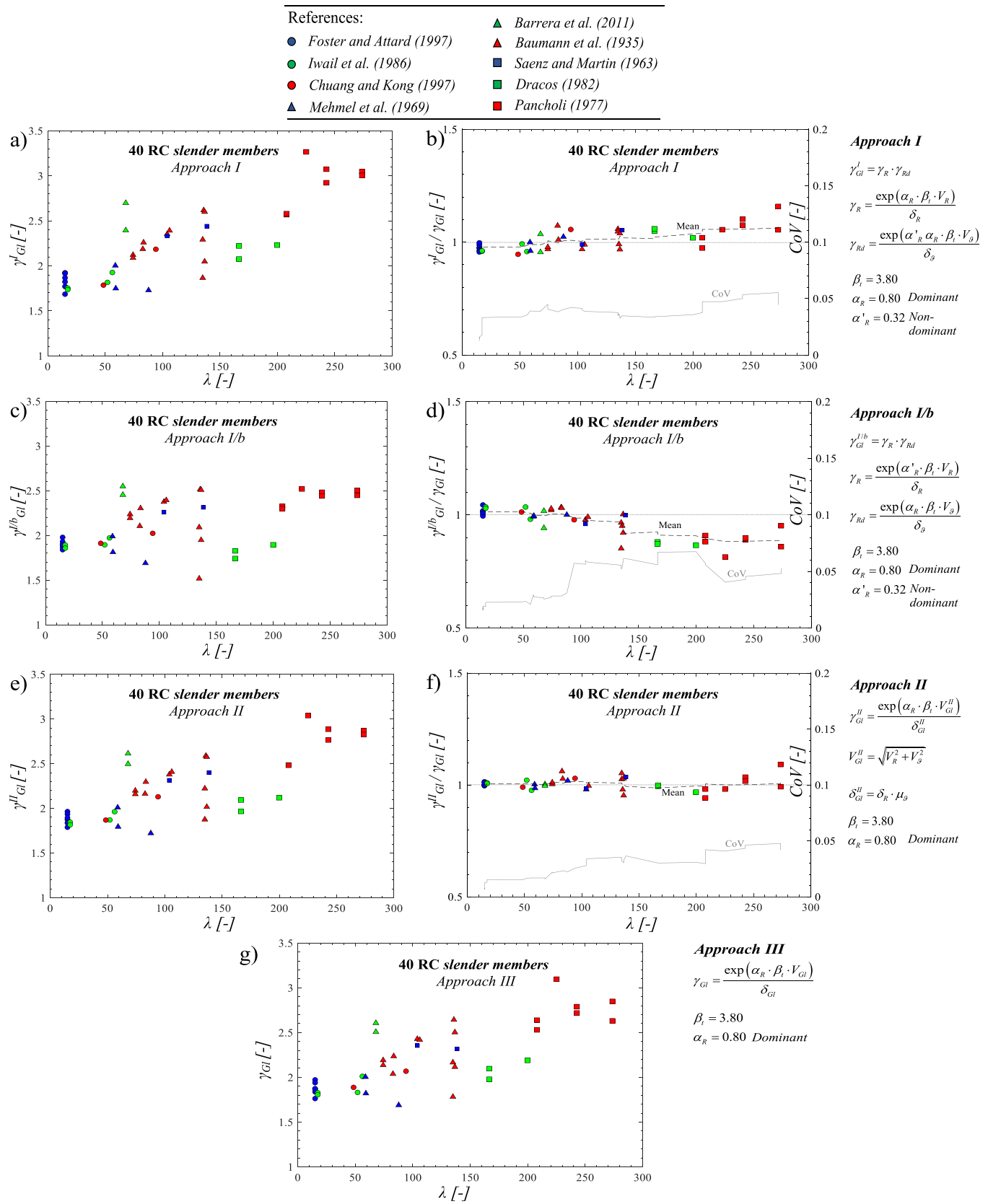

Fig. 7. 40 RC *slender members* [37–45]: global safety factors γ_{GI} related to *Approach I* (a), *I/b* (c), *II* (e) and *III* (g); comparison of *Approach I* (b), *I/b* (d), *II* (f) with *Approach III* - target level of reliability set to β_t= 3.8.

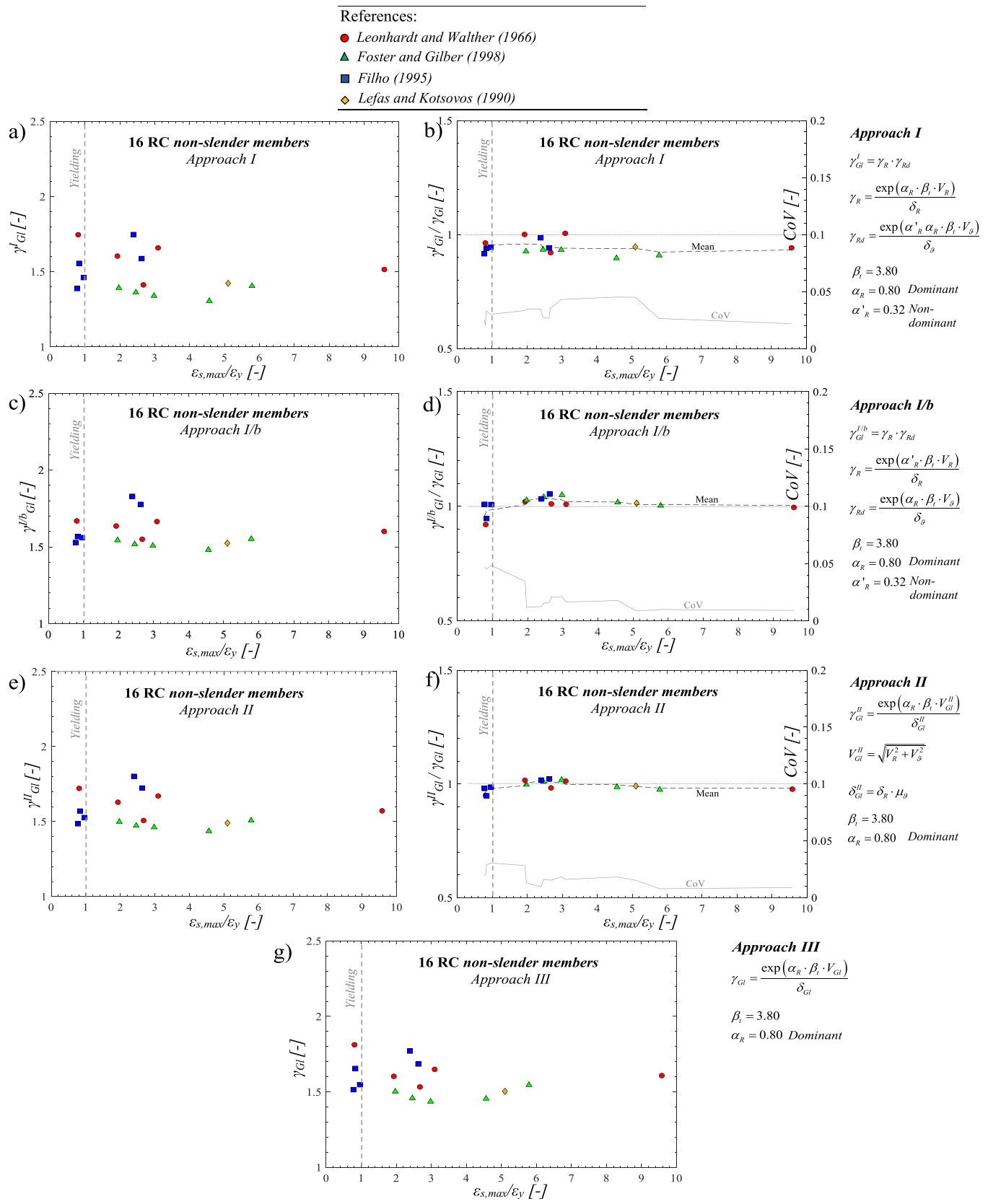

Fig. 8. 16 RC *non-slender members* [46–49]: global safety factors γ_{GI} related to *Approach I* (a), *I/b* (c), *II* (e) and *III* (g); comparison of *Approach I* (b), *I/b* (d), *II* (f) with *Approach III* - target level of reliability set to β_t= 3.8.

(2) without an explicit evaluation of the dominant or non-dominant role of the uncertainties. *Approach I* and *Approach I/b* have provided safer results in case of slender and non-slender systems, respectively. Although *Approach I* and *Approach I/b* need the assessment of the dominant role assumed by the uncertainties, they offer the enhancement of "easy-of-use" of the GRM with respect to *Approach II* for practical applications. This advantage stems from the possibility to assign fixed values of γ_{Rd} corresponding to specific reliability targets. These values can be derived from statistical assessments of model uncertainty [10,55,57,58,56]. This feature allows for their consistent use within various safety formats proposed by design codes [10,13] and scientific literature [15,30,33] and does not require to the practitioner to deal with statistical characterization of model uncertainty but only with the assessment of the value of γ_R.

6. Conclusions

This study evaluates various methodologies within the GRM for assessing the global safety factors of RC structures, employing a comprehensive set of probabilistic analyses to compare different approaches - *Approach I* (and *I/b*), *Approach II* and *Approach III* - across different RC structural members. The evaluation accounts for both aleatory (i.e., material properties and geometry) and epistemic (i.e., model) uncertainties. *Approach I* distinguishes between these uncertainties, assuming the aleatory ones dominant in the estimation of the global safety factor. *Approach I/b*, differently from *Approach I*, adopts the epistemic uncertainties as dominant. *Approach II* balances the significance of both uncertainties in the estimation of global safety factors. *Approach III* conducts a comprehensive probabilistic analysis for the global safety factor, incorporating both uncertainties to assess the global structural resistance, thus serving as the reference method for evaluating the effectiveness of other approaches.

A benchmark dataset of 56 experimental tests with 40 slender RC columns (having different slenderness ratios) and 16 non-slender RC components (i.e., walls, deep beams and shear walls) has been compiled since it represents a broad spectrum of structural behaviours and failure modes. NLN models for all 56 elements have been developed, using modelling assumptions aimed at optimizing alignment between numerical predictions and experimental results. Assuming specific probabilistic assumptions for aleatory and epistemic uncertainties, the detailed probabilistic analysis delves into how different sources of uncertainties affect the global behaviour of structural systems. The analysis reveals that, within the global assessment using NLNAs, the assumption that aleatory uncertainties dominate over epistemic ones is not always verified, especially, for non-slender members characterized by ductile failure mechanisms. In the last situations, the assumption of dominant epistemic uncertainties leads to safer results. A further finding is the robust performance of *Approach II*, which consistently outperforms other approaches in accuracy, irrespective of the uncertainties involved and their significance in affecting the global structural resistance and the nature of the failure mechanism. On the opposite, *Approach I* and *I/b* allow for "easy-of-use" of the GRM within design codes specifications with respect to *Approach II* even if they need to identify the dominant or non-dominant role of the uncertainties and, for instance, the nature of the failure mechanism as examined with reference to slender and non-slender RC members. Further investigations are needed to extend and confirm the mentioned above considerations beyond slender (i.e., columns) and non-slender (i.e., walls, deep beams) RC members, also considering RC members experiencing failures in bending and shear, such as beams, as well as slabs exhibiting punching failure modes. The implications of this research highlight both the positive and negative aspects associated with the available approaches for assessing global safety factors within the GRM. The aim is to facilitate a conscious and informed use of these approaches in the development of the next generation of design codes.

CRediT authorship contribution statement

Elena Miceli: Writing – review & editing, Writing – original draft, Visualization, Validation, Supervision, Software, Methodology, Investigation, Formal analysis, Data curation, Conceptualization. **Diego Gino:** Writing – review & editing, Writing – original draft, Visualization, Validation, Supervision, Software, Methodology, Investigation, Formal analysis, Data curation, Conceptualization. **Paolo Castaldo:** Validation, Supervision, Methodology, Investigation, Conceptualization.

Declaration of Competing Interest

No conflict of interest.

Data Availability

Data will be made available on request.

Acknowledgements

This study was carried out within the *Ministerial Decree no. 1062/2021* and received funding from the FSE REACT-EU - PON Ricerca e Innovazione 2014–2020. This manuscript reflects only the authors' views and opinions, neither the European Union nor the European Commission can be considered responsible for them.

This work is part of the collaborative activity developed by the authors within the Commission 3 – Task Group 3.1: *"Reliability and safety evaluation: full-probabilistic and semi-probabilistic methods for existing structures"* of the International Federation for Structural Concrete (*fib*).

This work is also part of the collaborative activity developed by the authors within the framework of the *WP 11 – Task 11.4 – ReLUIS*.

This study was also carried out within the "*Data fusion based digital twins for structural safety assessment*" project – funded by European Union – Next Generation EU within the PRIN 2022 program (D.D. 104 - 02/02/2022 Ministero dell'Università e della Ricerca). This manuscript reflects only the authors' views and opinions and the Ministry cannot be considered responsible for them.

Annex A

Annex A illustrates the 'empirical' and 'theoretical' CDFs concerning the global structural resistance of the GRRVs R and R_{Gl}. The figures encompass data for the 40 RC *slender members* [37–45] (Figure A3 and Figure A4) and 16 RC *non-slender members* [46–49] (Figures A5).

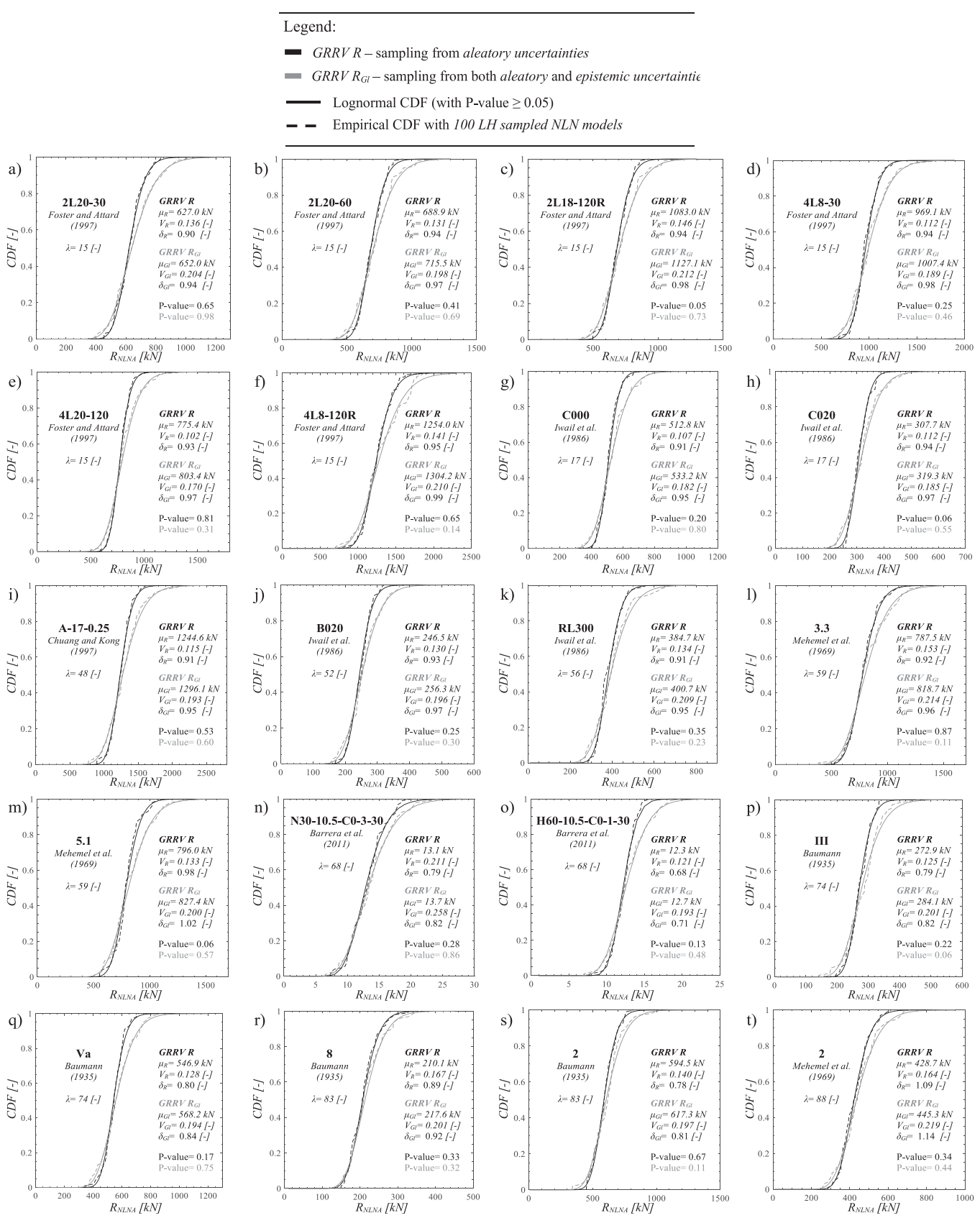

Fig. A1. 'Empirical' CDFs and related 'theoretical' lognormal CDFs of the GRRVs R and R_{Gl}, fitted by the ML method, for the RC *slender members* from references [37–45] (slenderness range from 15 to 88).

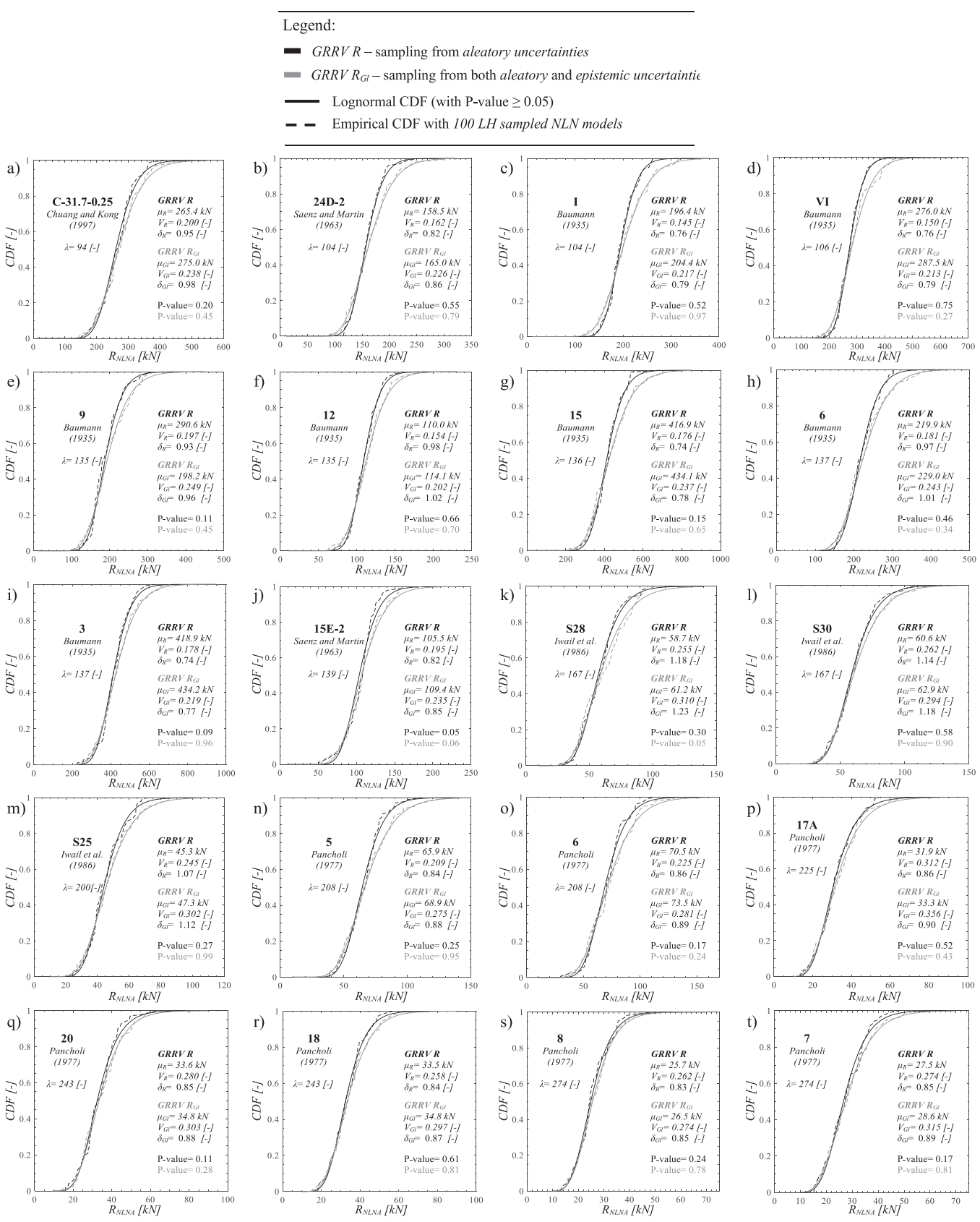

Fig. A2. 'Empirical' CDFs and related 'theoretical' lognormal CDFs of the GRRVs R and R_{Gl}, fitted by the ML method, for the RC *slender members* from references [37–45] (slenderness range from 94 to 274).

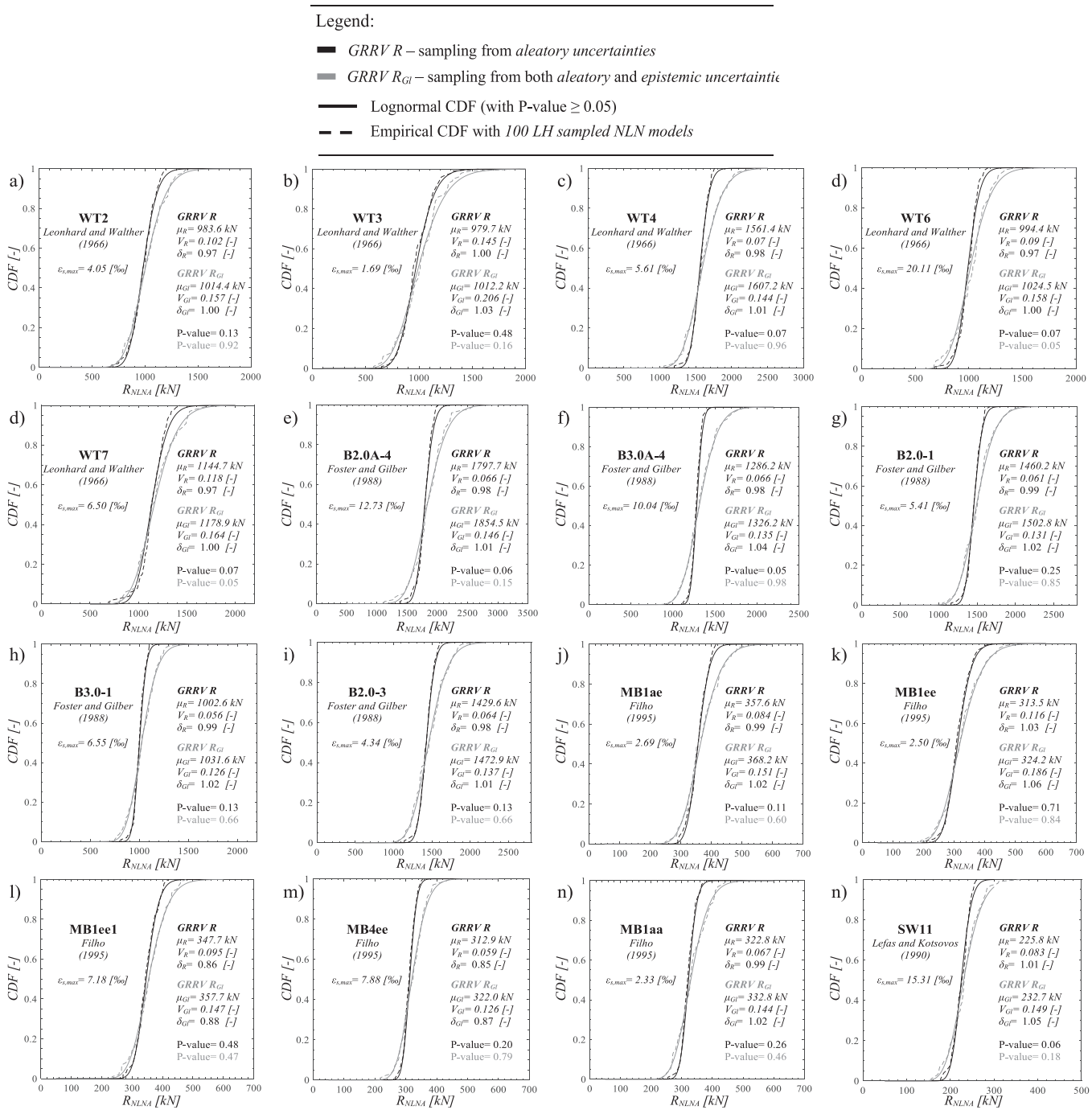

Fig. A3. 'Empirical' CDFs and related 'theoretical' lognormal CDFs of the GRRVs R and R_{Gl}, fitted by the ML method, for the group of RC *non-slender members* from references [46–49].

.

Annex B.

Annex B groups, in the Tables B1 and B2, the results in terms of the global safety factors and design value of the global structural resistance with reference to *Approach I*, *I/b*, *II* and *III* for the 40 RC *slender members* [37–45] and 16 RC *non-slender members* [46–49], respectively.

Table B1
Results for global safety factors and design value of global structural resistance (R_d) with reference to the *Approach I*, *I/b*, *II* and *III* for the 40 RC *slender members* [37–45].

Ref.	Exp. test	Type	λ [-]	*Approach I* (*aleatory uncertainty dominant*)				*Approach I/b* (*epistemic uncertainty dominant*)				*Approach II*		*Approach III*	
				β_t= 3.8											
				α'_R= 0.32	α_R= 0.80	γ^I_{Gl} [-]	R^I_d [kN]	α_R= 0.80	α'_R= 0.32	γ^I_{Gl} [-]	R^I_d [kN]	α_R= 0.80	R^{II}_d [kN]	α_R= 0.80	R^{III}_d [kN]
				γ_{Rd} [-]	γ_R [-]			γ_{Rd} [-]	γ_R [-]			γ^{II}_{Gl} [-]		γ^{III}_{Gl} [-]	
[37]	2L20-30	*B*	15		1.67	1.92	361.0	1.52	1.30	1.98	350.9	1.96	353.4	1.97	352.1
	2L20-60			1.15	1.58	1.82	404.0		1.25	1.90	388.4	1.87	393.0	1.87	393.7
	2L8-120R				1.66	1.92	601.4		1.27	1.93	597.4	1.94	595.6	1.94	594.3
	4L8-30				1.53	1.77	583.3		1.23	1.87	552.1	1.84	562.1	1.84	562.0
	4L20-120				1.46	1.69	492.8		1.21	1.84	451.5	1.79	464.6	1.76	471.2
	4L8-120R				1.62	1.87	706.5		1.25	1.90	695.8	1.89	696.6	1.87	704.4
[38]	C000	*A*	17		1.52	1.75	319.7		1.25	1.89	296.3	1.84	303.9	1.83	306.8
	C020	*B*			1.50	1.74	189.2		1.22	1.86	176.8	1.82	180.9	1.81	181.9
	B020		52		1.57	1.82	145.2		1.25	1.89	139.2	1.87	141.0	1.83	144.0
	RL300		56		1.67	1.93	219.7		1.30	1.97	214.6	1.96	215.7	2.01	210.5
[39]	A-17-0.25	*B*	48		1.55	1.79	765.6		1.26	1.91	715.3	1.87	731.7	1.89	724.3
	C-31.7-0.25		94		1.89	2.18	128.2		1.33	2.02	138.4	2.13	131.5	2.07	135.4
[40]	3.3	*B*	59		1.74	2.00	427.6		1.31	1.99	430.5	2.01	426.2	2.00	427.3
	5.1				1.52	1.75	463.4		1.19	1.81	447.5	1.79	452.0	1.82	445.3
	4.1		88		1.50	1.73	427.6		1.11	1.69	430.5	1.72	426.2	1.69	427.3
[41]	N30-10.5-C0-3-30	*C*	21		2.34	2.70	6.2		1.62	2.45	6.8	2.61	6.4	2.61	6.4
	H60-10.5-C0-1-30				2.07	2.39	7.5		1.68	2.55	7.0	2.50	7.2	2.51	7.1
[42]	III	*A*	74		1.84	2.12	163.7		1.47	2.24	155.3	2.20	158.0	2.19	158.5
	Va				1.81	2.09	325.9		1.45	2.19	310.3	2.16	315.2	2.14	318.7
	2		83		1.89	2.19	108.3		1.39	2.10	112.5	2.16	109.5	2.04	116.2
	I		104		1.96	2.26	337.4		1.52	2.30	330.8	2.30	331.8	2.24	340.8
	VI		106		2.04	2.35	109.7		1.57	2.38	108.6	2.38	108.5	2.43	106.2
	15		136		2.07	2.39	151.9		1.58	2.39	151.7	2.41	150.8	2.42	150.2
	3		137		1.99	2.29	89.9		1.38	2.09	98.5	2.22	92.7	2.17	95.1
	8		83		1.62	1.87	60.1		1.00	1.52	73.9	1.88	59.8	1.78	62.9
	9	*B*	135		2.27	2.62	214.1		1.66	2.51	222.9	2.59	216.5	2.64	212.0
	12				1.77	2.05	111.2		1.28	1.95	116.8	2.02	112.9	2.12	107.5
	6		137		2.25	2.60	216.7		1.65	2.51	224.6	2.57	218.8	2.50	225.1
[43]	24D-2	*D*	104		2.02	2.33	82.7		1.49	2.26	85.3	2.31	83.3	2.35	81.9
	15E-2	*A*	139		2.12	2.44	53.0		1.53	2.31	55.9	2.40	53.9	2.32	55.8
[44]	S28	*B*	167		1.80	2.08	24.0		1.15	1.74	28.6	1.97	25.4	1.98	25.2
	S30				1.92	2.22	24.0		1.20	1.83	29.2	2.09	25.5	2.10	25.5
	S25		200		1.93	2.23	18.9		1.25	1.89	22.3	2.12	19.9	2.19	19.3
[45]	5	*A*	208		2.23	2.57	30.6		1.53	2.32	33.9	2.48	31.7	2.64	29.8
	6				2.24	2.58	31.9		1.52	2.30	35.8	2.48	33.1	2.53	32.5
	17 A		225		2.83	3.27	11.4		1.66	2.52	14.7	3.04	12.2	3.10	12.0
	20		243		2.66	3.07	30.6		1.64	2.48	33.9	2.89	31.7	2.79	29.8
	18				2.53	2.92	31.9		1.61	2.44	35.8	2.77	33.1	2.72	32.5
	8		274		2.64	3.05	11.4		1.65	2.50	14.7	2.87	12.2	2.63	12.0
	7				2.60	3.00	30.6		1.61	2.45	33.9	2.83	31.7	2.85	29.8

(-)[*1]: constant value of the axial load applied to the column during the experimental test.

Table B2
Results for global safety factors and design value of global structural resistance (R_d) with reference to the *Approach I*, *I/b*, *II* and *III* for the 16 RC *non-slender members* [46–49].

Ref.	Exp. test	$\varepsilon^{*I}_{s,max}$ [-]	*Approach I* (*aleatory uncertainty dominant*)				*Approach I/b* (*epistemic uncertainty dominant*)				*Approach II*		*Approach III*	
			β_t= 3.8											
			α'_R= 0.32	α_R= 0.80	γ^I_{Gl} [-]	R^I_d [kN]	α_R= 0.80	α'_R= 0.32	γ^I_{Gl} [-]	R^I_d [kN]	α_R= 0.80	R^{II}_d [kN]	α_R= 0.80	R^{III}_d [kN]
			γ_{Rd} [-]	γ_R [-]			γ_{Rd} [-]	γ_R [-]			γ^{II}_{Gl} [-]		γ^{III}_{Gl} [-]	
[46]	WT2	$4.05\bullet10^{-3}$	1.12	1.43	1.60	629.5	1.40	1.17	1.64	617.5	1.64	620.1	1.60	630.0
	WT3	$1.69\bullet10^{-3}$		1.55	1.75	561.1		1.19	1.67	587.4	1.67	569.4	1.81	540.7
	WT4	$5.62\bullet10^{-3}$		1.26	1.41	1125.2		1.11	1.55	1026.2	1.55	1055.0	1.53	1036.9
	WT6	$2.01\bullet10^{-2}$		1.35	1.52	673.0		1.14	1.60	637.3	1.60	649.0	1.61	634.2
	WT7	$6.50\bullet10^{-3}$		1.48	1.66	711.2		1.19	1.66	709.0	1.66	706.4	1.65	715.4
[47]	B2.0A-4	$1.27\bullet10^{-2}$		1.25	1.41	1308.9		1.11	1.55	1186.4	1.55	1220.9	1.55	1190.2
	B3.0A-4	$1.00\bullet10^{-2}$		1.16	1.31	980.5		1.06	1.48	864.5	1.48	891.3	1.46	879.4
	B2.01	$5.41\bullet10^{-3}$		1.21	1.36	1078.6		1.08	1.52	969.2	1.52	998.4	1.46	1007.9
	B3.01	$6.55\bullet10^{-3}$		1.19	1.34	753.7		1.08	1.51	670.2	1.51	690.8	1.44	703.3

(*continued on next page*)

Table B2 (*continued*)

Ref.	Exp. test	$\varepsilon^{*1}_{s,max}$ [-]	*Approach I* (*aleatory uncertainty dominant*)				*Approach I/b* (*epistemic uncertainty dominant*)				*Approach II*		*Approach III*	
			β_t= 3.8											
			α'_R= 0.32	α_R= 0.80	γ^I_{GI} [-]	R^I_d [kN]	α_R= 0.80	α'_R= 0.32	γ^I_{GI} [-]	R^I_d [kN]	α_R= 0.80	R^{II}_d [kN]	α_R= 0.80	R^{III}_d [kN]
			γ_{Rd} [-]	γ_R [-]			γ_{Rd} [-]	γ_R [-]			γ^{II}_{GI} [-]		γ^{III}_{GI} [-]	
	B2.03	$4.34\bullet10^{-3}$		1.24	1.39	1048.6		1.10	1.54	946.2	1.54	974.3	1.50	971.6
[48]	MB1ae	$2.69\bullet10^{-3}$		1.30	1.46	246.3		1.12	1.56	230.8	1.56	235.8	1.55	232.5
	MB1ee	$2.50\bullet10^{-3}$		1.38	1.56	196.0		1.12	1.57	194.6	1.57	194.3	1.66	184.3
	MB1ee1	$7.18\bullet10^{-3}$		1.56	1.75	231.8		1.31	1.83	221.5	1.83	224.9	1.77	228.7
	MB4ee	$7.88\bullet10^{-3}$		1.41	1.59	233.0		1.27	1.78	208.4	1.78	214.7	1.69	219.5
	MB1aa	$2.33\bullet10^{-3}$		1.24	1.39	234.1		1.09	1.53	212.7	1.53	218.8	1.51	214.5
[49]	SW11	$1.53\bullet10^{-2}$		1.27	1.42	156.3		1.09	1.52	146.0	1.52	149.3	1.50	148.0

(-)^{*1}: maximum strain attained in the primary reinforcement in NLNAs conducted with experimental material and geometrical properties.

References

[1] De Matteis G, Caprili S, Carbonari S, Chisari C, D'Amato M, Mattei F, et al. Critical issues in safety assessment of existing reinforced concrete bridges by means of nonlinear analysis. Procedia Struct Integr 2023;44:681–8.

[2] Lara C, Tanner P, Zanuy C, Hingorani R. Reliability verification of existing RC structures using partial factors approaches and site-specific data. applied sciences 2021;11(4):1653.

[3] Vecchi F, Belletti B. Capacity assessment of existing RC columns. Buildings 2021;11 (4):161. https://doi.org/10.3390/buildings11040161.

[4] Abdel-Rahman AM, El-Din AS, El-Gawad HA. A review of nonlinear finite element analysis methods for reinforced concrete structures. Structures 2021;28:102034.

[5] Dudziak S. Numerically efficient three-dimensional model for non-linear finite element analysis of reinforced concrete structures. Materials 2021;14:1578.

[6] Ftima Mehdi Ben, Massicotte Bruno. Utilization of nonlinear finite elements for the design and assessment of large concrete structures. I: calibration and validation. J Struct Eng 2015;141(9):04014217. https://doi.org/10.1061/(ASCE)ST.1943-541X.0001160.

[7] Bagge N. Demonstration and examination of a procedure for successively improved structural assessment of concrete bridges. Struct Concr 2019:1–24.

[8] Ftima MB, Massicotte B. Development of a reliability framework for the use of advanced nonlinear finite elements in the design of concrete structures. J Struct Eng 2012;138:1054–64.

[9] CEN. EN 1992–1-1: Eurocode 2 – Design of concrete structures. Part 1–1: general rules and rules for buildings. CEN 2014. Brussels.

[10] fib Model Code for Concrete Structures 2010. fib 2013. Lausanne.

[11] fib Bulletin N°45 . Practitioner's guide to finite element modelling of reinforced concrete structures – State of the art report. Lausanne; 2008.

[12] Guidelines for Nonlinear Finite Element Analysis of Concrete Structures, Rijkswaterstaat Technical Document (RTD), Rijkswaterstaat Centre for Infrastructure RTD: 1016–1:2020, 2020.

[13] prEN 1992-1–1:2021 Eurocode 2 – Design of concrete structures. Brussels.

[14] Castaldo P, Gino D, Mancini G. Safety formats for non-linear analysis of reinforced concrete structures: discussion, comparison and pr.oposals. Eng Struct 2019;193: 136–53. https://doi.org/10.1016/j.engstruct.2018.09.041.

[15] Cervenka V. Reliability-based non-linear analysis according to *fib* Model Code 2010. Struct Concr 2013;14(1):19–28.

[16] Most T. Assessment of structural simulation models by estimating uncertainties due to model selection and model simplification. Comput Struct 2011;89(17-18): 1664–72.

[17] Bratina S, Saje M, Planinc I. On materially and geometrically non-linear analysis of reinforced concrete planar frames. Int J Solids Struct 2004;Volume 41(Issues 24–25):7181–207. https://doi.org/10.1016/j.ijsolstr.2004.06.004.

[18] Miceli E, Castaldo P. Robustness improvements for 2D reinforced concrete moment resisting frames: parametric study by means of NLFE analyses. 2024 Struct Concr 2024;25:9–31. https://doi.org/10.1002/suco.202300443.

[19] Slobbe A, Rózsás _A, Allaix DL, Bigaj-van Vliet A. On the value of a reliability-based nonlinear finite element analysis approach in the assessment of concrete structures. Struct Concr 2019:1–16. https://doi.org/10.1002/suco.201800344.

[20] Mohammed A, Almansour H, Martín-Pérez B. Simplified finite element model for evaluation of ultimate capacity of corrosion-damaged reinforced concrete beam-columns. Int J Adv Struct Eng 2018;10:381–400. https://doi.org/10.1007/s40091-018-0204-2.

[21] Belletti B., Scolari M., Vecchi F. PARC_CL 2.0 crack model for NLFEA of reinforced concrete structures under cyclic loadings. Computer and Structures 191: 165–179.

[22] Ferrara M, Gino D, Miceli E, Giordano L, Malavisi M, Bertagnoli G. Safety assessment of existing prestressed RC bridge decks through different approaches. Struct Concr 2024. https://doi.org/10.1002/suco.202301049.

[23] Bouchaboub M, Samai ML. Nonlinear analysis of slender high-strength R/C columns under combined biaxial bending and axial compression. Eng Struct 2013; 48:37–42.

[24] Zhang Mingyang, Song Huijuan, Lim Sopokhem, Akiyama Mitsuyoshi, Frangopol Dan M. Reliability estimation of corroded RC structures based on spatial variability using experimental evidence, probabilistic analysis and finite element method. Eng Struct 2019;Volume 192:30–52. https://doi.org/10.1016/j.engstruct.2019.04.085.

[25] Mankar Amol, Bayane Imane, Sørensen John Dalsgaard, Brühwiler Eugen. Probabilistic reliability framework for assessment of concrete fatigue of existing RC bridge deck slabs using data from monitoring. Eng Struct 2019;Volume 201: 109788. https://doi.org/10.1016/j.engstruct.2019.109788.

[26] Lara C, Tanner P, Zanuy C, Hingorani R. Reliability verification of existing RC structures using partial factors approaches and site-specific data. Appl Sci 2021;11 (4):1653. https://doi.org/10.3390/app11041653.

[27] Yu Q, Ruiz MF, Muttoni A. Considerations on the partial safety factor format for reinforced concrete structures accounting for multiple failure modes. Eng Struct 2022;264:114442.

[28] CEN. EN 1990: Eurocode – Basis of structural design. CEN 2013. Brussels.

[29] Castaldo P, Gino D, Marano GC, Mancini. G. Aleatory uncertainties with global resistance safety factors for non-linear analyses of slender reinforced concrete columns. Eng Struct 2022;255:113920.

[30] Allaix DL, Carbone VI, Mancini G. Global safety format for non-linear analysis of reinforced concrete structures. Struct Concr 2013;14(1):29–42.

[31] ISO 2394. General principles on reliability for structures. Genéve. 2015.

[32] fib Bulletin N°80 . Partial factor methods for existing concrete structures, Lausanne, Switzerland; 2016.

[33] Tur Viktar V, et al. Safety formats for non-linear analysis: are the current structural codes applicable for practice? (Aug). Solid State Phenomena, vol. 309. Trans Tech Publications, Ltd.; 2020. p. 193–200. https://doi.org/10.4028/www.scientific.net/ssp.309.193 (Aug).

[34] Hasofer A.M., Lind N.C. Exact and invariant second moment code format, Journal of the Engineering Division ASCE 1974; 100(EM1): 111–121.

[35] König G., Hosser D. The simplified level II method and its application on the derivation of safety elements for level I.CEB; 1982.

[36] Yu Q, Valeri P, Ruiz MF, Muttoni A. A consistent safety format and design approach for brittle systems and application to textile reinforced concrete structures. Eng Struct 2021;249(2021):113306. https://doi.org/10.1016/j.engstruct.2021.113306.

[37] A. Mehmel, H. Schwarz, K.H. Karperek, and J. Makovi. Tragverhalten ausmittig beanspruchter stahlbetondruckglieder. institut für baustatik, eht, deutscherausschuss für stahlbeton, heft 204, 1969.

[38] Luis P. Saenz and Ignacio Martin. Test of reinforced concrete columns with high slenderness ratios. In Journal Proceedings, volume 60, pages 589–616, 1963.

[39] Foster Stephen J, Attard Mario M. Experimental tests on eccentrically loaded high strength concrete columns. Struct J 1997;94(3):295–303.

[40] V.R. Pancholi. The Instability of Slender Reinforced Concrete Columns. PhD thesis, University of Bradford, 1977.

[41] Adriana Dracos. Long slender reinforced concrete columns. PhD thesis, University of Bradford, 1982.

[42] S..IwaiI, K. Minami, and M. Wakabayashi. Stability of slender reinforced concrete columns subjected to biaxially eccentric loads, 1986.

[43] Chuang PH, Kong FK. Large-scale tests on slender, reinforced concrete columns. Struct Eng 1997;75(23):410–6.

[44] Barrera AC, Bonet JL. Manuel L Romero, and PF Miguel. Experimental tests of slender reinforced concrete columns under combined axial load and lateral force. Eng Struct 2011;33(12):3676–89.

[45] Oskar Baumann. Die Knickung der Eisenbeton-Säulen. PhD thesis, ETH Zurich, 1935.

[46] Leonhardt F, Walther RWandartige Träger. Deutscher Ausschuss für Stahlbeton. Heft 178. Berlin. Germany: Ernst & Sons; 1966.

[47] Foster SJ, Gilbert J. Experimental studies on high strength concrete deep beams. Acids Struct J 1998;95:382–90.

[48] Filho J.B. Dimensionamento e comportamento do betao estrutural em zonas com discontinuitades. PhD thesis. Universidade Tecnica de Lisbona 1995.

[49] Lefas ID, Kotsovos MD. Behaviour of reinforced concrete structural walls: strength, deformation characteristics and failure mechanism. Acids Struct J 1990;87:23–31.
[50] Gino D, Castaldo P, Giordano L, Mancini G. Model uncertainty in non-linear numerical analyses of slender reinforced concrete members. Struct Concr 2021; 22.2:845–70.
[51] Gino D, Miceli E, Castaldo P, Recupero A, Mancini G. Strain-based method for assessment of global resistance safety factors for NLNAs of reinforced concrete structures. Eng Struct 2024:117625. https://doi.org/10.1016/j.engstruct.2024.117625.
[52] JCSS. 2001 JCSS Probabilistic Model Code.
[53] fib Model Code for Concrete Structures 2020. fib 2024. Lausanne.
[54] Castaldo P, Gino D, Carbone VI, Mancini G. Framework for definition of design formulations from empirical and semi-empirical resistance models. 2018 Struct Concr 2018;19(4):980–7. https://doi.org/10.1002/suco.201800083.
[55] Castaldo P, Gino D, Bertagnoli G, Mancini G. Partial safety factor for resistance model uncertainties in 2D non-linear analysis of reinforced concrete structures. Eng Struct 2018;176:746–62. https://doi.org/10.1016/j.engstruct.2018.09.041.
[56] Engen M, Hendriks MAN, Monti G, Allaix DL. Treatment of modelling uncertainty of NLFEA in *fib* Model Code 2020. Structural Concrete, 22; 2021. p. 3202–12. https://doi.org/10.1002/suco.2021004203212ENGENETAL.
[57] Engen M, Hendriks MAN, Köhler J, Øverli JA, Åldtstedt E. A quantification of modelling uncertainty for non-linear finite element analysis of large concrete structures. Struct Saf 2017;64:1–8.
[58] Castaldo P, Gino D, Bertagnoli G, Mancini G. Resistance model uncertainty in non-linear finite element analyses of cyclically loaded reinforced concrete systems. Eng Struct 2020;211(2020):110496. https://doi.org/10.1016/j.engstruct.2020.110496.
[59] Blomfors M, Engen M, Plos M. Evaluation of safety formats for non-linear finite element analyses of statically indeterminate concrete structures subjected to different load paths. Struct Concr 2016;17(1):44–51.
[60] Kadlec L, Červenka V. Model uncertainties of FEM nonlinear analyses of concrete structures. Solid State Phenom 2016;249:197. -20.
[61] Shlune H, Gylltoft K, Plos M. Safety format for non-linear analysis of concrete structures. Mag Concr Res 2012;64(7):563–74.
[62] Yu Q, Simoes JT, Muttoni A. Model uncertainties and partial safety factors of strain-based approaches for structural concrete: Example of punching shear. Eng Struct 2023;292(2023):116509.
[63] Holický M, Retief JV, Sikora M. Assessment of model uncertainties for structural resistance. Probabilistic Eng Mech 2016;45:188–97.
[64] Sykora M, Holicky M, Prieto M, Tanner P. Uncertainties in resistance models for sound and corrosion-damaged RC structures according to EN1992-1-1. Mater Struct 2014;48:34153430.
[65] Taerwe RL. Towards a consistent treatment of model uncertainties in reliability formats for concrete structures. CEB Bull d'Information 1993;(No 105-S17):5–34.
[66] ACI318-19. Building Code Requirements for Structural Concrete. Farmington Hills, MI, USA: American Concrete Institute; 2019.
[67] Engen M, Hendriks MAN, Øverli JA, Åldtstedt E. Solution strategy for non-linear finite element analyses of large reinforced concrete structures. Str Concr 2015;3: 389–97.
[68] Belletti B, Damoni C, Hendriks MAN. Development of guidelines for nonlinear finite element analyses of existing reinforced and prestressed beams. Eur J Environ Civ Eng 2011;15(9):1361–84.
[69] McKenna F, Fenves GL, Scott MH. Open system for earthquake engineering simulation. Berkeley, CA: University of California,; 2000.
[70] Murat Saatcioglu, Razvi Salim R. Strength and ductility of confined concrete. J Struct Eng 1992;118(6):1590–607.
[71] Chang, G. and Mander, J. (1994). "Seismic Energy Based Fatigue Damage Analysis of Bridge Columns: Part I – Evaluation of Seismic Capacity." NCEER Technical Report 94–0006.
[72] Dhakal R, Maekawa K. Modeling for postyield buckled of reinforcement. J Struct Eng 2002;128(9):1139–47.
[73] ATENA 2D v5.9 . 2022. Cervenka Consulting s.r.o. Prague. Czech Republic.
[74] Faber MH. Statistics and Probability Theory. Springer; 2012.
[75] Mckey MD, Conover WJ, Beckman RJ. A comparison of three methods for selecting values of input variables in the analysis from a computer code. Technometrics 1979;21:239–45.
[76] Anderson TW, Darling DA. Asymptotic theory of certain "goodness-of-fit" criteria based on stochastic processes. Ann Math Stat 1952;23:193–212.
[77] Faber. Michael Havbro Statistics and Probability Theory. Springer; 2012.
[78] Hastie T, Tibshirani R, Friedman JH. The elements of statistical learning. New York, NY: Springer; 2009.
[79] Teichgräber Max, Köhler Jochen, Straub Daniel. Hidden safety in structural design codes. Eng Struct 2022;Volume 257:114017.